Host, Suppressor and Promoter – the Roles of Ni and Fe on Oxygen Evolution Reaction Activity and Stability of NiFe Alloy Thin Films in Alkaline Media

Fuxi Bao,[a,*] Erno Kemppainen,[a] Iris Dorbandt,[a] Fanxing Xi,[a] Radu Bors,[a] Natalia Maticiuc,[a] Robert Wenisch,[a] Rory Bagacki,[a] Christian Schary,[a] Ursula Michalczik,[b] Peter Bogdanoff,[b] Iver Lauermann,[a] Roel van de Krol,[b] Rutger Schlatmann,[a] and Sonya Calnan[a]

[a]PVcomB, Helmholtz-Zentrum Berlin für Materialien und Energie GmbH, Schwarzschildstrasse 3, 12489 Berlin, Germany

[b]Institute for Solar Fuels, Helmholtz-Zentrum Berlin für Materialien und Energie GmbH, Hahn-Meitner-Platz 1, 14109 Berlin, Germany

Tel.: +49 (30) 8062-15572, Fax: +49–30–8062–15677

fuxi.bao@helmholtz-berlin.de

Abstract

Understanding the oxygen evolution reaction (OER) activity and stability of the NiFe-based materials is important for achieving low-cost and highly efficient electrocatalysts for practical water splitting. Here, we report the roles of Ni and Fe on the OER activity and stability of metallic NiFe and pure Ni thin films in alkaline electrolyte. Our results support that the $Ni(OH)_2$/NiOOH does not contribute to the OER directly, but it serves as an ideal host for Fe incorporation, which is essential for obtaining high OER activity. Furthermore, the availability of Fe in the electrolyte is found to be important and necessary for both NiFe and pure Ni thin films to maintain enhanced OER performance, while the presence of Ni is detrimental to the OER kinetics. The impacts of Fe and Ni species present in KOH on the OER activity are consistent with the dissolution/re-deposition mechanism we propose. Stability studies show that as long as Fe (both co-electrodeposited Fe and incorporated Fe) is present in the electrocatalyst film, the OER activity will degrade under prolonged continuous operation. Satisfactory stability can, however, be achieved with intermittent OER operation in which the catalyst cycles between a degraded and recovered state. Accordingly, two important ranges, i.e., the recovery range and the degradation range, are proposed. Prolonged continuous OER operation (i.e. in the degradation range) generates NiOOH in the electrocatalyst which likely enhances the formation of FeOOH and eventually leads to the OER deactivation. If the electrode works in the recovery range for a certain period, i.e., at a sufficiently low reduction potential, where the Ni^{3+} is reduced to Ni^{2+}, the OER activity can be maintained (and even improved).

Key words: OER, NiFe, thin film, dissolution/re-deposition, stability

1. Introduction

The generation of hydrogen through water splitting is considered a promising route for storing energy from intermittent renewable sources such as solar, wind, and tidal energy.[1,2] Since one of the main energy losses in water splitting is the kinetic overpotential of the oxygen evolution reaction (OER),[3,4] OER electrocatalysts have been extensively investigated in order to improve the efficiency of water splitting. Noble metal oxides, such as RuO_2 and IrO_2, have been proven to exhibit high catalytic activity toward the OER.[3,5] However, the scarcity and high cost of these noble metals largely hinder their large-scale application. Thus, the development of earth-abundant electrocatalysts with low cost and high efficiency is critical.

Mixed Ni-Fe based materials have been reported as the most active earth-abundant electrocatalysts for OER in alkaline water electrolysis.[6,7] Although it is widely accepted that the interaction between Ni and Fe is significant for enhancing the OER activity,[8] their roles for the OER activity are still debated.[9,10] Various forms of NiFe-based materials, such as alloys,[11,12] oxides,[13] and oxyhydroxides,[14,15] have been studied as OER electrocatalysts for alkaline water splitting. Among them, the alloys have attracted attention because of the simplicity of their preparation by electrodeposition and strong adhesion to the substrate.[13,16] However, the as-prepared structure of NiFe alloys is not the active phase for OER catalysis and therefore, an electrochemical activation step is usually required to convert the metallic/oxide phase to (oxy)hydroxide in order to achieve better OER activity.[10,16,17] Unlike NiFe (oxy)hydroxides, which have been thoroughly investigated as OER electrocatalysts, few studies have been conducted on NiFe-based alloys.[10,17,18] The electrochemical behavior and the surface structural evolution of NiFe-based alloys in alkaline media under OER operating conditions remain unclear and still need further investigations.[16]

A concern about NiFe-based materials is their stability. Although significant effort has been devoted to developing highly active NiFe-based OER electrocatalysts, few studies have focused on the topic of stability,[19–23] which is also important for practical water splitting. Recent studies show that degradation is a common issue among the NiFe-based electrocatalysts under prolonged OER conditions, but the causes are still not fully understood.[19,20,22,24] For example, Speck *et al.* found that the Fe in the $FeNiO_x$ films (anode), which were synthesized via electrodeposition or near-infrared driven decomposition, leached into the KOH electrolyte and was deposited on the Ni-cathode during the OER, which is likely related to the OER degradation especially at high current densities.[21] Obata *et al.* also observed the loss of Fe from

electrodeposited $NiFeO_x$ films (on an Au-coated FTO substrate) into the KOH electrolyte during the OER, which resulted in gradual OER deactivation with time.[22] Additionally, the existing stability studies on NiFe-based OER electrocatalysts have mainly concentrated on NiFe-(oxy)hydroxides. Since NiFe alloys would experience a surface change from a metallic/oxide to a hydroxide/(oxy)hydroxide during the OER, which is different from pure Ni-Fe (oxy)hydroxide because this is an active phase towards OER itself,[25] further studies are needed to clarify the details about the OER stability of NiFe alloys. Specifically, what electrochemical/chemical conditions can cause degradation, how the structure changes during the degradation, and if and how the degradation can be restored/maintained.

Recently, the dissolution/re-deposition of metallic species has been proposed to explain the dynamic metal ion exchange between the catalyst surface and the electrolyte during the OER process.[26–29] Anantharaj *et al.* observed a change in faceting of crystallographic planes from (001) to (101) and (202) planes for nickel hydroxide after cyclic voltammetry (CV) treatment and they ascribed it to the re-deposition of nickel ions during OER.[30] Ye *et al.* reported that $Ni(OH)_2$/NiOOH film suffered from chemical dissolution, evidenced by the presence of Ni(II) species in NaOH electrolyte observed with in situ UV-vis spectroscopy.[31] Chung *et al.* reported that the surface Fe, regardless of its phase/oxidation state, is not stable in KOH and always dissolves in aqueous KOH during the OER operation, which leads to reduced activity of the electrocatalyst.[26] They also found that to maintain the OER activity, certain amount of Fe in KOH is necessary to continuously compensate for the Fe dissolved from the electrocatalyst surface via a Fe dissolution/re-deposition process. Therefore, they suggested that the dynamically stable Fe is the active site for OER and keeping the balance between the dissolution rate and re-deposition rate is significant to maintain the OER activity and stability of Fe-MO_xH_y (M=Ni, Co, Fe). Kuai *et al.* recently studied the stability of the NiFe-hydroxide and suggested that the decay in catalytic activity under prolonged continuous OER is caused by phase segregation due to the Fe dissolution/re-deposition process.[29] Therefore, operation at the reducing potential for Ni could mitigate the phase segregation and avoid the decay in OER activity. However, the details of the dissolution/re-deposition process remain unclear, e.g., how does the Fe and/or the Ni concentration in the alkaline electrolyte affect the dissolution and re-deposition rate, and how do the operating conditions affect the OER activity and stability.

In this contribution, we provide new insights into the roles of Fe and Ni in both metallic NiFe (and pure Ni thin) films and KOH electrolytes toward OER activity and stability. We first study the surface structural evolution and its influence on OER activity of the thin films in the

presence and absence of Fe in the KOH. We further perform a series of experiments by varying the concentration of the Ni and Fe species in the KOH electrolyte to understand the roles of Ni and Fe on the OER activity of the NiFe and pure Ni thin films. Based on the achieved results, we propose a dissolution/re-deposition mechanism for the Ni and Fe species present in KOH. Using continuous and intermittent OER operation, we show that two potential ranges can be distinguished for the OER stability, apparently divided by the $Ni(OH)_2$/NiOOH redox potential. Lastly, a simple but reasonable hypothesis is proposed to explain the OER degradation and preservation with respect to the existing form of Fe in the film which is likely linked with the Ni valence state that affects the stability.

2. Experimental

2.1 Chemical and materials

$NiSO_4 \cdot 6H_2O$ (≥99.99%, Carl Roth GmbH + Co. KG), nickel nitrate (99.9985%, Alfa Aesar), $Na_3C_6H_5O_7 \cdot 2H_2O$ (≥99.0%, Sigma-Aldrich), iron(II) sulfate heptahydrate (99.999%, ALORICH), iron(III) nitrate nonahydrate (99+%, Acros Organics), potassium hydroxide pellets (EMPLURA®, Merck KGaA), and 20% ammonia solution (analytical reagent, VWR International) were used without any further purification. All electrolyte solutions were prepared with 18.2 MΩ cm de-ionised (DI) water obtained from a water purification system (Barnstead Smart2Pure 3 from ThermoFisher Scientific). For all depositions and analytical experiments, glass substrates coated with SnO_2:F (FTO) of ~8.6 Ω/sq sheet resistance were used as the working electrode.

2.2 Preparation of KOH electrolytes

All electrolytes used in this work for catalytic study are 1.0 M KOH. The unpurified KOH was prepared by using the KOH pellets listed in section 2.1. For this KOH, the Fe and Ni concentrations are 1.38 and 0.31 μmol L^{-1}, respectively, determined by inductively coupled plasma-optical emission spectroscopy (ICP-OES, Table S1). The purified KOH was obtained by purifying the unpurified KOH according to the procedure described by Trotochaud *et al.*[32] and the resulting Fe and Ni concentrations were determined as 0.45 and 16.43 μmol L^{-1}, respectively. In addition, two groups of KOH solutions containing various Ni and Fe concentrations were prepared by adding a certain amount of nickel nitrate and iron(III) nitrate solutions, respectively.

2.3 Electrodeposition of NiFe alloy films on FTO

Typically, a 500 mL electrochemical bath for electrodeposition consisting of 0.024 M $NiSO_4 \cdot 6H_2O$, 0.006 M $FeSO_4 \cdot 7H_2O$ and 0.030 M $Na_3C_6H_5O_7$ was used. The pH of the bath was adjusted to 10.0 using 20% ammonia solution. The electrodeposition was done in a three-electrode configuration. A 6 × 5 cm^2 nickel foil (thickness: 0.5 mm, Alfa Aesar, 99.94%) and an Ag/AgCl electrode (METTLER TOLEDO) filled with 3.0 M KCl were employed as the counter electrode and the reference electrode, respectively, while 1 × 3 cm^2 FTO substrates were used as working electrodes. All the FTO substrates were masked off with Kapton tape to expose a 1 × 1 cm^2 area for deposition.

Electrodeposition of NiFe films was performed at a current density of –12 mA cm^{-2} for 20 s at room temperature (~25°C) using Biologic potentiostat (SP-150). After the deposition, the obtained NiFe films were rinsed several times with DI water and then dried with nitrogen gas. The electrodeposition of pure Ni films was prepared on the same sized FTO substrate in a similar electrolyte but without the addition of iron(II) sulfate heptahydrate. The electrodeposition was conducted at –12 mA cm^{-2} for 40 s.

2.4 Characterization methods

2.4.1 Material characterization

The structure of the as-prepared electrocatalysts on FTO was characterized by grazing incidence X-ray diffraction (GIXRD) using a Bruker AXS D8 Advance X–ray diffractometer with Cu Kα radiation (λ = 0.15406 nm). The angle of incidence for the GIXRD measurement was controlled to be 0.25° and the step size was 0.02 with step time of 2 s. The surface morphology of the films was characterized by field emission scanning electron microscopy (FESEM) using a LEO GEMINI 1530 instrument from ZEISS at 50 k magnification and 5 kV acceleration voltage. The surface composition of the film surface was determined by X-ray Photoelectron Spectroscopy (XPS) in the CISSY-set-up at the BESSY II synchrotron in Berlin, details of which can be found elsewhere.[33] For all measurements performed in this study, Mg Kα excitation with an energy of 1253.6 eV was used. XPS fine spectra were recorded with a pass energy of 20 eV, with the exception of the Fe 2p, which was recorded with E_{pass} = 50 eV to get a better signal-to-noise ratio. The corresponding change in the Fe sensitivity was taken into account for the quantitative analysis. The Raman spectra were recorded using a custom-made system from S&I components (Germany) equipped with a frequency-doubled Nd:YAG laser emitting light at a wavelength of λ = 532 nm. During the measurement, the exposure time was set to be 60 s and 10 exposures were accumulated per spectrum. The thicknesses of the NiFe

and pure Ni films on FTO after deposition were determined with a stylus profilometer (Dektak XT, Bruker).

2.4.2 Electrochemical characterization

The electrochemical characterization was conducted in an H-cell with the two chambers separated by a Zirfon membrane (Provided by AGFA) in order to avoid the crossover of H_2 and O_2. The working and reference electrodes were placed in one chamber and the counter electrode in the other. An Hg/HgO (Fisherbrand™ accumet™) electrode filled with 1.0 M KOH was employed as the reference electrode while a 3 × 4 cm^2 graphite plate (Alfa Aesar) was used as the counter electrode. All electrochemical measurements were carried out using Biologic SP-150 potentiostat at room temperature, and in all measurements the stirring rate was controlled to be 600 rpm.

Cyclic voltammetry (CV) was performed in the potential range of 0–0.8 V vs Hg/HgO at a scan rate of 100 mV s^{-1} or 20 mV s^{-1}. The activation procedure consisted of 3 CV cycles at 20 mV s^{-1} followed by 200 CV cycles at 100 mV s^{-1} and finally 3 CV cycles at 20 mV s^{-1}. The electrochemical impedance spectroscopy (EIS) measurements were conducted in the frequency range of 100 kHz–0.1 Hz with 10 mV amplitude under an applied potential of 0.6 V vs Hg/HgO. Before each EIS recording, the working electrode was held at 0.6 V vs Hg/HgO for 60 s to ensure a stable current.

The stability measurements were conducted using the chronoamperometry technique by three different protocols: (1) fixing the applied potential at 1.725 V_{RHE} for 48 hours; (2) fixing the potential at 1.725 V_{RHE} for 10 min and then at 1.225 (or 1.445) V_{RHE} for another 10 min, and cycling between these two potentials for 48 h (144 cycles); (3) controlling the potential in a cycle between 1.725 V_{RHE} for 10 min, 10 min at the potential of 1.575 V_{RHE}, and then the open circuit potential (OCP) for another 10 min, with a total duration of 96 hours (192 cycles). The purpose of the first protocol was to perform a continuous OER operation while the second and third ones were used to mimic the varying, cyclic operation of an intermittent renewable energy supply.

3. Results and discussion

3.1 Morphology and structure of as-prepared NiFe and pure Ni films

Electrodeposition was used to prepare electrocatalytic NiFe and pure Ni thin films for the OER. The films show strong adhesion to the FTO substrates (Figure S1) and provide a suitable

platform to investigate the OER activity and stability. The SEM images (Figure 1a) show that the NiFe films consist of uniform small particles of ~40 nm diameter and that the particles homogeneously cover the FTO substrate, while the Ni film in Figure 1b is also very uniform and its surface consists of smaller particles (diameter ca. 10 nm). The phase structure of the freshly prepared thin films was characterized using grazing incidence X-ray diffraction (GIXRD) and Raman spectroscopy. As shown in Figure 1c, the diffraction peaks marked with the hash symbol "#" are indexed to tin oxide, SnO_2, with crystalline tetragonal structure (ICDD, PDF No. 00-041–1445). The appearance of diffraction peak positioned at 44.7° (marked with the asterisk symbol "*") for NiFe film is attributed to the (111) plane of crystalline NiFe.[34,35] Similarly, there is only one characteristic peak located at 44.7° for the pure Ni film, indicating that the film is phase-pure (ICDD, PDF No. 00-001–1258).[36] The Raman spectra of the NiFe and pure Ni films were collected in the wavenumber range of 100 cm^{-1} to 900 cm^{-1} (Figure 1d). The appearance of a characteristic signal at 533 cm^{-1} for the Ni film can be ascribed to the stretching mode of the Ni-O bond and is generally considered to be evidence for oxide film formation on metallic Ni-alloys.[37,38] The shift of the wavenumber of the Ni-O bond to 552 cm^{-1} for the NiFe film is likely caused by the presence of co-deposited Fe due to the co-deposited Fe. The GIXRD and Raman results indicate that the surface of the NiFe and pure Ni films have been oxidized to some extent although the bulk of the films remains in the metallic phase.

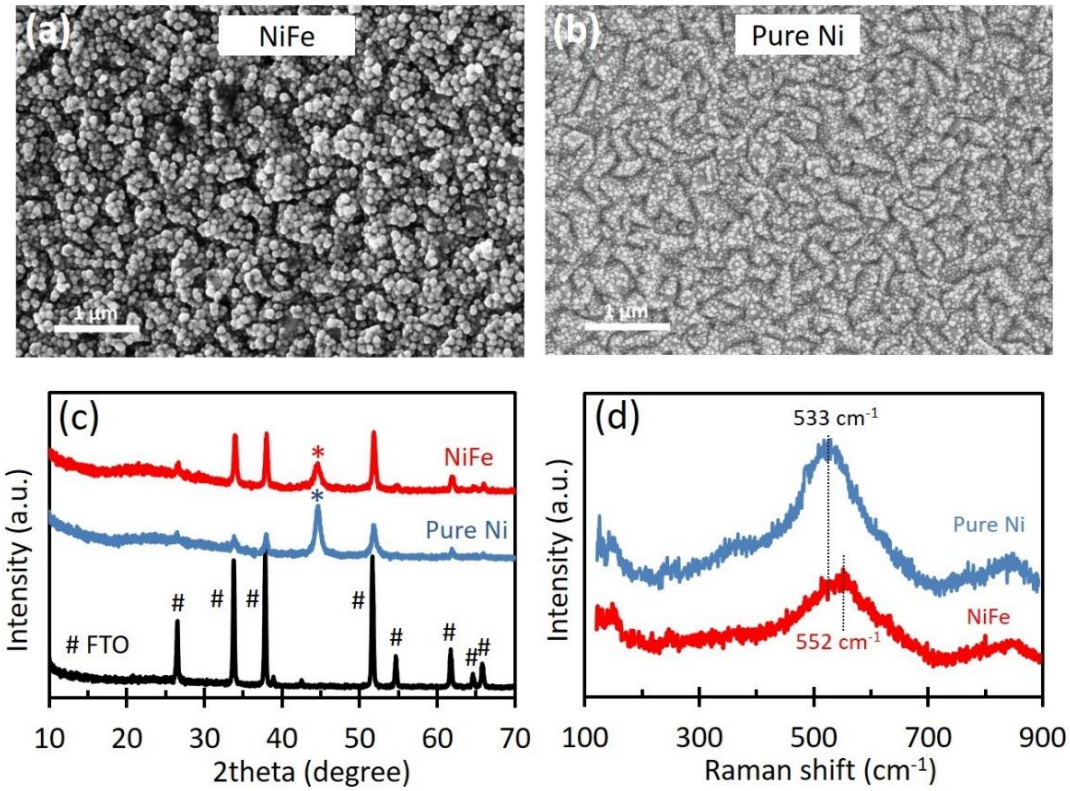

Figure 1. (a, b) SEM images of NiFe and pure Ni films; (c) GIRXD patterns and (d) Raman spectra of NiFe and pure Ni films.

3.2 CV activation and surface evolution

It has been reported that the surface of pure Ni is very sensitive to alkaline electrolyte and can be easily oxidized to $Ni(OH)_2$ even without applied potential.[39,40] Under OER operation, the Ni^0 and Fe^0 in NiFe will be oxidized into high-valence Ni/Fe oxides and (oxy)hydroxides.[18] Unlike NiFe (oxy)hydroxides, which have been proven to be OER-active, metallic NiFe will first experience a surface phase evolution in alkaline media under OER conditions. Furthermore, Fe is important for achieving enhanced OER activity for Ni-based electrocatalysts,[41] although how it affects the OER activity remains unclear. Herein, we first electrochemically analyzed the NiFe and pure Ni thin films in unpurified and purified KOH electrolytes. In this work, the unpurified KOH refers to the freshly prepared 1.0 M KOH by using KOH pellets, while the purified KOH refers to 1.0 M KOH which was treated according to Trotochaud *et al.* (see Section 2.2).[32] Due to the redox feature of Ni, the cyclic voltammetry (CV) measurement contains information about also the phase change in addition to the OER activity of the films.[42]

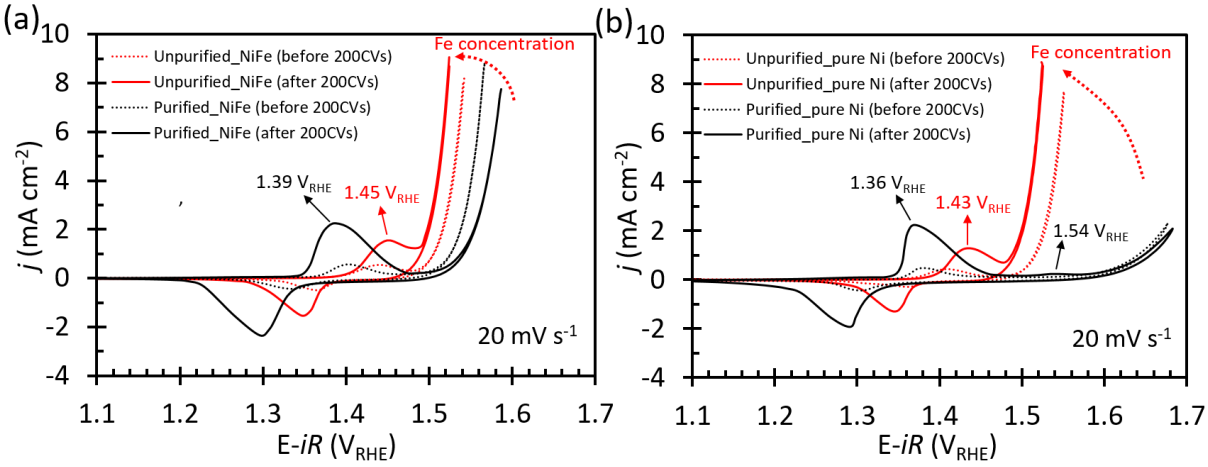

Figure 2. CVs of NiFe films (a) and pure Ni films (b) collected in unpurified KOH and purified KOH at the scan rate of 20 mV s^{-1}.

Figure 2 shows the CV curves of the NiFe and pure Ni films before and after 200 CVs. Both in unpurified or purified KOH, the size of the Ni redox feature for both films is very small in the first cycles, indicating that only a small fraction of the films is oxidized/reduced initially.[43] This is in accordance with the GIXRD and Raman results in Figure 1, in which only the metallic and oxide phases were detected. After 200 CVs, the height of the redox feature in all the KOH

electrolytes has significantly increased, suggesting that more metallic Ni was oxidized to Ni^{2+}/Ni^{3+}, which can be described as:[44]

$$Ni^0 \leftrightarrow Ni^{2+} + 2e^- \quad (1)$$

$$Ni(OH)_2 + OH^- \leftrightarrow NiOOH + H_2O + e^- \quad (2)$$

It is noted that the oxidation peak of the films in unpurified KOH is located at a ~60 mV more anodic potential, i.e., 1.45 V_{RHE}, than for films in purified KOH (1.39 V_{RHE}). This can be explained by the partial charge transfer effect due to the incorporation of Fe from unpurified KOH.[32] This is supported by the smaller size of redox feature in unpurified KOH compared to that in purified KOH, because the presence of Fe partially suppressed the oxidization of the Ni.[45] The CV results of pure Ni films also exhibit the same trends in terms of Ni redox feature size and position (Figure 2b), with about 20–30 mV less anodic peak positions as for NiFe. The appearance of the feature at 1.54 V_{RHE} in purified KOH (black curve) is ascribed to the formation of Ni^{4+}.[32]

Regarding the OER activity, the improved OER activity of NiFe and pure Ni films in unpurified KOH after the CV cycling could be due to the incorporation of Fe.[46] Surprisingly, the OER activity of pure Ni reaches that of NiFe after 200 CVs (overpotential of 290 mV at 8 mA cm^{-2}). This result indicates that an enhanced OER activity can be obtained by modifying the surface of the pure Ni film with Fe-containing KOH. It is noticeable that the increase in $Ni(OH)_2$/NiOOH content after 200 CVs does not directly contribute to the OER because the overpotential of the pure Ni sample in purified KOH does not decrease (although after the CV treatment the size of the redox feature increases significantly). This is consistent with the incorporation of Fe being the main cause of the improved activity.[43,47] Even so, the increased $Ni(OH)_2$/NiOOH content still plays an important role in improving the OER activity. As shown in Figure S2, after one hour of OER (@10 mA cm^{-2}) or OCP operation in unpurified KOH, the size of redox feature has only slightly increased, as did the OER activity. However, after cycling for one hour (=200 CV cycles) in unpurified KOH, the size of the redox feature has increased significantly (i.e. more $Ni(OH)_2$/NiOOH generated) and the OER activity has greatly improved. These results suggest that the $Ni(OH)_2$/NiOOH mixed phase is a better host for Fe incorporation than the nickel oxide/metallic Ni structure. In addition, the OER activity of NiFe in purified KOH decreases with CV cycling, while that of the pure Ni is poor and remains almost unchanged. Pure NiO_x has already been proven to be a very poor OER electrocatalyst.[48] The poor OER activity of pure Ni in purified KOH proves the importance of Fe for the OER. The deactivation of NiFe in purified KOH after 200 CVs indicates that even for a NiFe film, the

presence of additional Fe ions in the electrolyte is essential in order to maintain the OER activity. These results are consistent with the recent report by Halaoui *et al.* where they found the Fe presence in electrolyte to be critical for the superior OER activity of $NiFeO_xH_y$.[28]

In some articles,[42,49] the integrated area of the Ni redox peak is considered to be proportional to the concentration of active surface sites (or electrochemically active surface area, ECSA). Our results show that although the area of the Ni redox peak for a pure Ni film increases significantly after 200 CVs in purified KOH, the OER activity remains almost unchanged. Thus, the integrated area of the Ni redox peak does not have a direct relationship with the OER activity and should not be used to calculate the concentration of OER-active surface sites.

In order to understand how the cyclic voltammetry experiments affect the surface phase/structure of the NiFe and pure Ni films as well as the OER activity, Raman spectroscopy was employed to track the phase change of the films ranging from the 1st CV to 200th CV (Figure 3). Note that the Raman spectra were collected immediately, i.e., within minutes, after the CV cycling. Song *et al.* reported that the NiOOH phase has a one hour life time under OCP conditions.[50] In the present work we found that the surface phase of NiFe film after the CV treatment can be stable in air for at least four hours (Figure S3). Therefore, the Raman spectra collected immediately after electrochemical tests should reflect the true surface condition of the films in KOH.

As shown in Figure 3, at the beginning of the cyclic voltammetry (i.e. after the 1st CV), two characteristic modes positioned at 480 and 557 cm^{-1} are observed for NiFe and pure Ni films due to the formation of NiOOH.[39,40] These two modes are ascribed to the depolarized E_g mode and the polarized $A1_g$ stretch vibration of the NiO_2 framework, respectively.[51] Also, the peaks in the Raman spectra of the films treated in the purified KOH solution are generally narrower and sharper than those of the corresponding films treated in the unpurified KOH, indicating fewer crystalline defects and consistent with a smaller number of incorporated impurities. It is noticeable that the intensities of both I_{480} and I_{557} increase with increasing number of CV cycles. Note that the I_{557}/I_{480} ratio in this work is calculated based on the peak intensities of I_{557} and I_{480}. Since these two modes are associated with the NiOOH phase, the increase in intensity must be related to the formation of NiOOH deeper in the films.[40] This result is indeed consistent with the CV results in Figure 2, where the size of Ni redox peak, which is due to the formation of NiOOH (Eq. (2)), increases with the number of CV cycles. It is also observed that I_{480} increases faster with CV cycling compared to I_{557}, indicating a gradual structure change of the film. After 200 CVs the I_{557}/I_{480} ratio for NiFe and pure Ni films in unpurified KOH is higher than that for

the films treated in purified KOH. It has been reported that the I_{557}/I_{480} ratio has a close relationship with the Fe content in the film,[39,48] i.e., the increase in Fe content results in the increasing structural disorder of the film.[52,53] Normally the higher the Fe content, the higher value of the I_{557}/I_{480} ratio.

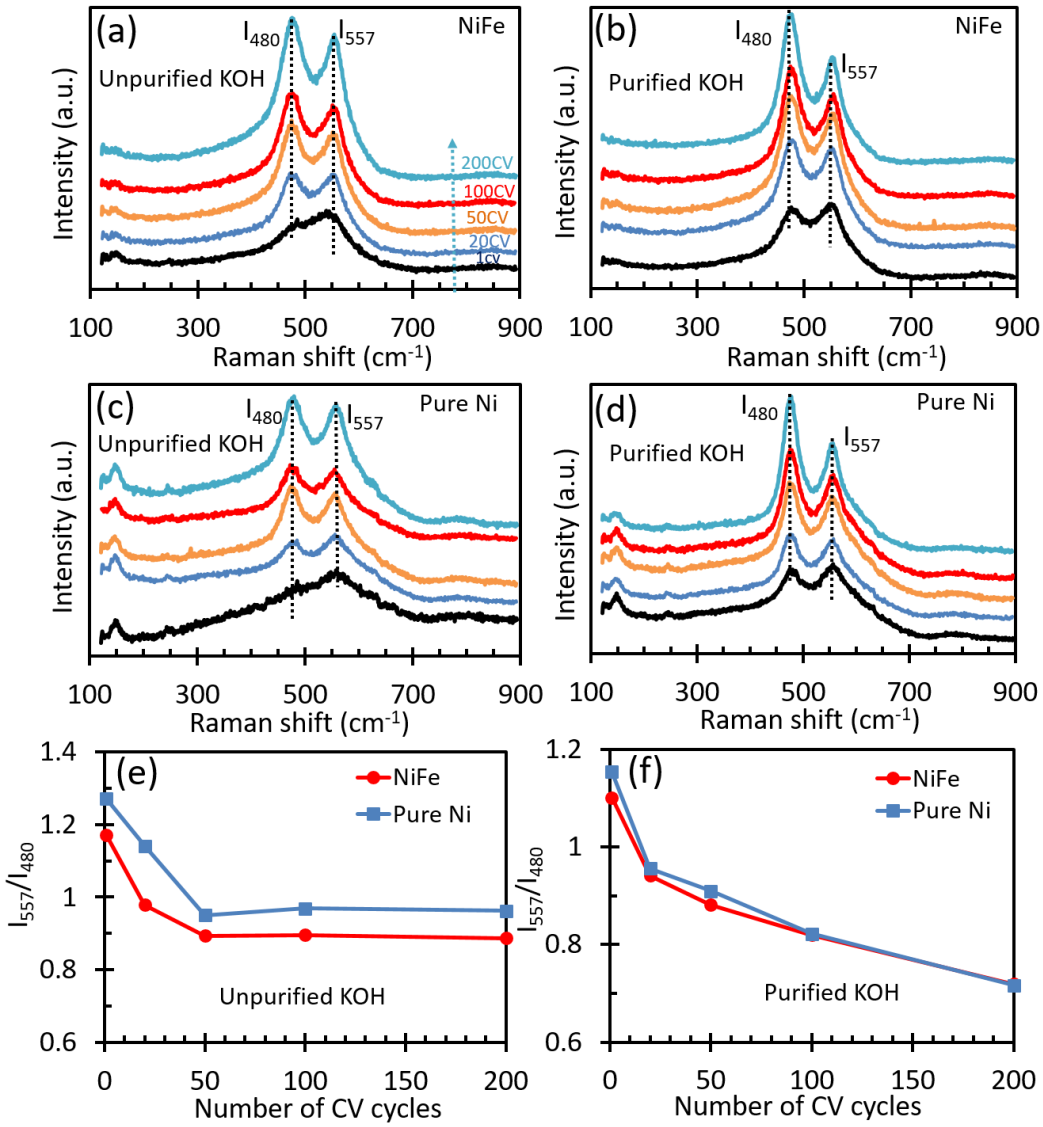

Figure 3. Raman spectra collected after various CV cycles for NiFe (a, b) and pure Ni films (c, d) in unpurified and purified KOH electrolytes; I_{557}/I_{480} ratio as a function of CV cycle number: (e) NiFe and pure Ni films in unpurified KOH and (f) NiFe and pure Ni films in purified KOH.

The I_{557}/I_{480} ratios as a function of CV cycle number are shown in Figure 3e and 3f. In unpurified KOH, the I_{557}/I_{480} value decreases within the first 100 CV cycles for both NiFe and pure Ni films, indicating that more NiOOH has formed on the film surface. The I_{557}/I_{480} value stabilizes after 100 CV cycles, suggesting that the Fe content on the catalyst surface has reached an equilibrium. However, in purified KOH, the I_{557}/I_{480} ratio continues to decrease with CV cycling,

indicating less Fe incorporation and more NiOOH formation on the surface. The GIXRD data for both NiFe and pure Ni films after 200 CV cycles was also collected. However, metallic phase still remains as the main structure of both (Figure S4), indicating that the CV treatment only transforms the surface of the films while the bulk remains metallic.[54] This is different from the NiFe-oxy(hydroxide) film, where the whole film is highly accessible to the electrolytes due to their layered-double hydroxide (LDH) structure which allows the intercalation of anions.[16] The comparison of the unpurified and purified KOH results suggests that Fe incorporated from KOH onto the catalyst surface during CV cycling not only affects the structure of the films (more disordered) but also the OER activity.

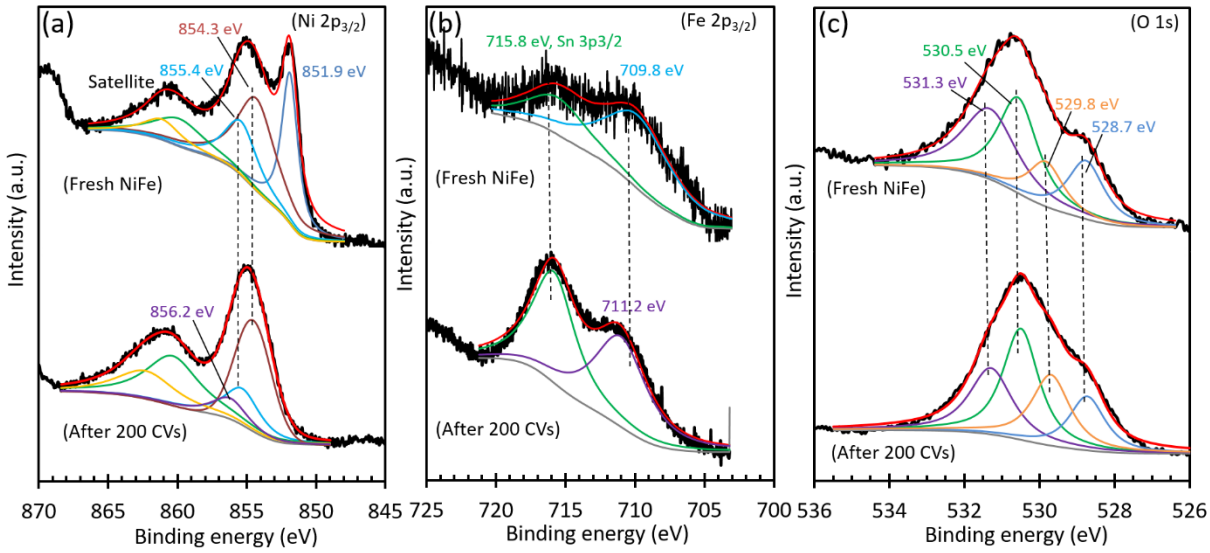

Figure 4. XPS spectra of Ni $2p_{3/2}$, Fe $2p_{3/2}$ and O 1s of freshly prepared NiFe and NiFe after 200 CV cycles in unpurified KOH.

XPS was used to study the chemical changes at the surface of the NiFe before (fresh NiFe) and after the 200 CVs in unpurified KOH (Figure 4) to understand the surface evolution caused by the CV treatment. For a freshly prepared NiFe film, the XPS peak derived from the high-resolution scan of Ni $2p_{3/2}$ (Figure 4a) can be resolved into three peaks located at 851.9 eV, 854.3 eV and 855.4 eV, which correspond to the metallic Ni, NiO and $Ni(OH)_2$ phases, respectively.[55] It is noted that the assignment of Ni 2p peaks to the valence states of Ni is always difficult due to the possible interference from the multiple contributions from Ni oxides and the satellite structures.[55,56] After 200 CVs, the peak corresponding to Ni^0 at 851.9 eV disappears, while a new peak at 856.2 eV is observed and can be ascribed to the formation of NiOOH, which is consistent with the Raman results where the characteristic peaks at 480 and 557 cm^{-1} are observed (Figure 3a). These results indicate the transformation of Ni^0/NiO/$Ni(OH)_2$ into $Ni(OH)_2$/NiOOH during the CV cycling. The XPS spectra of Fe $2p_{3/2}$ (Figure 4b) show that for

freshly prepared NiFe, the surface of the film contains a FeO (709.8 eV) phase.[57] However, after 200 CV cycles it disappears and a new peak at 711.2 eV appears, which can be attributed to the presence of Fe^{3+} in the form of Fe_2O_3 and/or Fe-oxy(hydroxide).[58] The characteristic binding energy at 715.8 eV belongs to the Sn $3p_{3/2}$ signal of the FTO substrate (Figure S12).[59] The XPS spectra of O 1s can be deconvoluted into four peaks at 528.7, 529.8, 530.5, and 531.3 eV. The peak at 528.7 eV is located at lower binding energies than normally found in NiO, but Hu *et al.* found a similar peak for a selenide-derived NiFe oxide that exhibited a layered structure.[60] The 529.8 eV peak can be ascribed to lattice oxygen in polycrystalline NiO, further confirming the existence of NiO.[61] The peak features positioned at 530.5 and 531.3 eV can be attributed to oxide and hydroxy groups of the NiFe alloy, respectively.[62] From the Ni and Fe spectra (Fig. 4a and 4b), we calculated that the Fe content (molar ratio of Fe/(Fe+Ni)) in unpurified KOH before CV cycling was 9.7 at.% and increased to 18.7 at.% after 200 CV cycles. These results further prove that the NiFe film absorbs Fe from the unpurified KOH electrolyte during CV cycling.

3.3 Impact of concentration of Fe and Ni species and dissolution/re-deposition mechanism

So far, we have studied the NiFe and pure Ni films in unpurified and purified KOH electrolytes. The results indicate that the surface evolution and the change of OER activity during the electrochemical activation are closely linked with the Fe species in KOH. This raises the question of how exactly the presence of Fe species in the KOH affects the as-prepared metallic thin film and the OER activity. Although the roles of Fe in alkaline media have been thoroughly investigated, few studies have systematically evaluated the impact of the Fe concentration on the OER activity.[26,27,31] More importantly, no mechanism has yet been proposed that explains how Fe is incorporated into the film from the alkaline electrolyte and how it is dissolved from the film into the electrolyte. Additionally, we are also curious about the impact of Ni species in the KOH, because it has been reported that the $Ni(OH)_2$/NiOOH suffers from chemical dissolution in alkaline conditions and the presence of Ni species deteriorates the OER activity.[31] This suggests that the existing studies in the literature on NiFe-based OER electrocatalysts under alkaline conditions might be (to a greater or lesser extent) affected by the Ni species in electrolyte.

Based on above considerations, we intend to study how the concentrations of the soluble Ni and Fe species in the KOH affect the OER activity of the thin films and the possible interaction between them. Thus, we prepared a series of 1.0 M KOH electrolytes with various Ni and Fe

concentrations and conducted the CV activation on the pure Ni thin films. Here, the use of pure Ni films instead of NiFe is to eliminate the impact of co-electrodeposited Fe.

Figure 5a shows the impact of various Ni concentrations in unpurified KOH on the OER activity. At low Ni concentration (1.0 μmol L^{-1}), the obtained CV curves before and after the 200 CVs almost overlap those in unpurified KOH (i.e. without the addition of Ni), indicating that such a low Ni concentration has almost no effect on the OER activity. However, as the Ni concentration is increased to 10 μmol L^{-1}, the OER activity drops significantly, even though it still improves during cycling (solid vs. dashed curves in Figure 5a). Our results prove that the presence of Ni in KOH indeed reduces the OER activity, probably by occupying the Fe sites. As the Ni concentration increases to 15 μmol L^{-1}, the OER activity reduces further and remains unchanged after 200 CVs, indicating that the dissolution/re-deposition between the Ni and Fe has reached a dynamic equilibrium. From the OCP-OES results (Table S1, Supporting Information), we know that the Fe concentration in unpurified KOH is 1.38 μmol L^{-1}. Since the Ni concentration needed to achieve a dynamic Ni/Fe equilibrium is ~10× higher, we deduce that the dissolution/re-deposition rate of Fe is around 10-fold that of Ni. Further increasing the Ni concentration (to 35 μmol L^{-1}) resulted in a worse OER activity (with little difference before and after cycling), suggesting that a high Ni concentration increases the deposition rate of Ni on the Fe sites, which suppresses the OER activity. This again indicates that the dissolution/re-deposition rate of Ni is much lower than that of Fe, which is consistent with some reports that the corrosion rate of Ni is low in KOH under OER operation.[29]

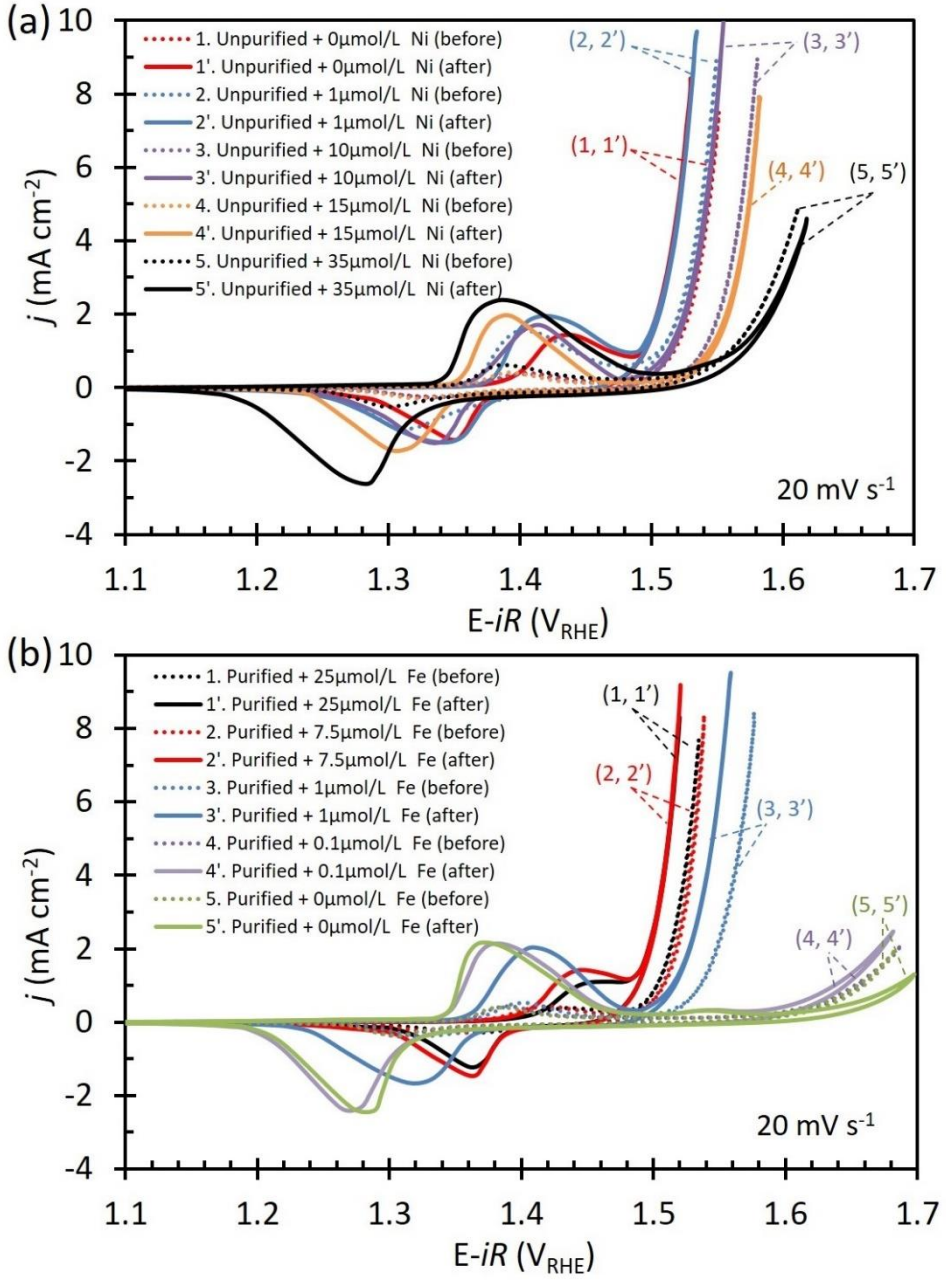

Figure 5. (a) CV curves of pure Ni films collected before and after 200 CV cycles in unpurified KOH with different Ni concentrations; (b) CV curves of pure Ni films collected before and after 200 CV cycles in purified KOH with different Fe concentrations.

The impact of the Fe concentration on the OER activity was also studied by varying the Fe content in the purified KOH (Figure 5b). Note that for purified KOH (without the addition of Fe) the original Fe and Ni concentrations are 0.45 and 16.43 µmol L^{-1}, respectively (Table S1, supporting information). By adding 0.1 µmol L^{-1} Fe to the purified KOH, the OER activity improves slightly. Even so, such Fe concentration (i.e. 0.55 µmol L^{-1} in total) is still too low to eliminate/offset the suppressive effect of the Ni species in the purified KOH. As the Fe concentration is increased by 1 µmol L^{-1}, the OER activity significantly improves, with further

improvement after cycling. Increasing the Fe concentration by 7.5 μmol L^{-1} further improved the OER activity. However, increasing the concentration by 25 μmol L^{-1} did not lead to further changes in the OER activity. It is noted that the OER activity achieved (overpotential of 292 mV at 8 mA cm^{-2}) in purified KOH with an added Fe concentration of 7.5 or 25 μmol L^{-1} after 200 CVs is close to that of pure Ni in unpurified KOH (overpotential of 290 mV at 8 mA cm^{-2}, Figure 5a). These results imply that the suppressive effect of Ni species in purified KOH can be completely eliminated by Fe species at a sufficiently high Fe concentration. The influence of the Fe concentration in KOH has been studied by Chung *et al.*, who reported that the OER enhancement by adding Fe to KOH saturates at around 0.1 ppm (~1.8 μmol L^{-1}, in purified KOH).[26] This value is different from our results and we assume that it should be determined for specific conditions such as the initial Ni/Fe ratio, the structural phase and specific surface area of the NiFe electrocatalyst, the applied potential, etc. In addition, compared to purified KOH with 7.5 μmol L^{-1} Fe, the smaller size of the anodic feature in the CV for purified KOH with 25 μmol L^{-1} Fe indicates that although more Fe is incorporated in the film from the KOH with high Fe concentration, the additional Fe does not increase the OER activity. These results suggest that not all the incorporated Fe from the KOH contributes to the OER. In other words, there must be a finite concentration of Fe active sites on the surface that should be determined by the film morphology, porosity, composition, etc.

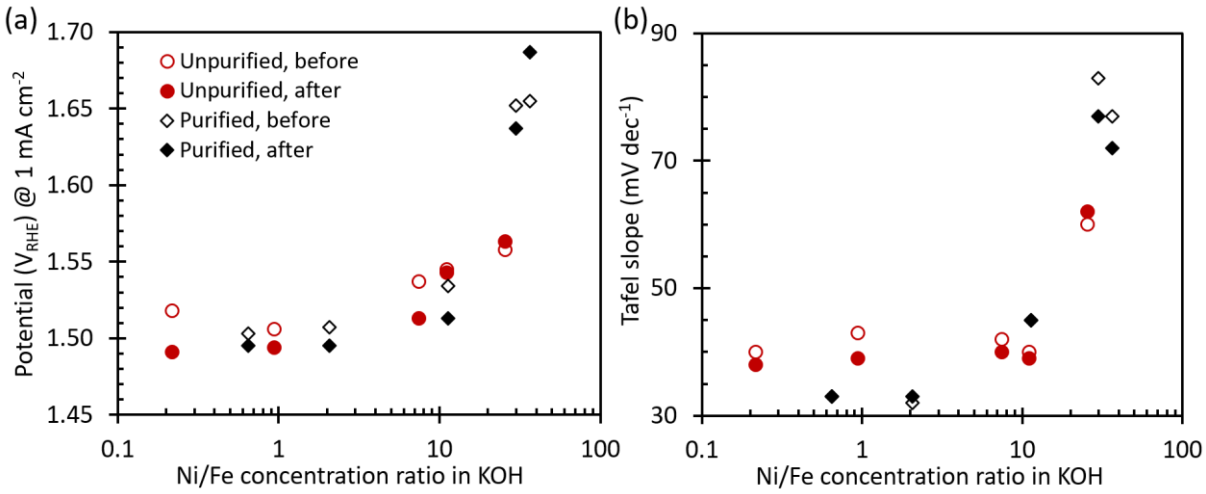

Figure 6. (a) The potential at 1 mA cm^{-2} current density and (b) Tafel-slope as function of the Ni/Fe concentration ratio in unpurified and purified KOH before and after 200 CVs.

Further quantification of the results in Figure 5 indicates that the concentration ratio of Ni/Fe (or Fe/Ni) is a very good descriptor for the OER activity. As shown in Figure 6, the data from both the purified and unpurified electrolytes essentially falls on the same curve when plotted as

a function of the concentration ratio, despite an order of magnitude difference in the absolute Fe and Ni concentrations for Ni/Fe ratios less than 2. Both the potential at 1 mA cm^{-2} and the Tafel slope exhibit the same general trend. The current density 1 mA cm^{-2} was chosen, because it was low enough that accurate potential could be determined for all measured CV curves. The highest performance is achieved with Ni/Fe ratio less than 2, and in those cases the OER performance appears nearly independent of the ratio. This matches the aforementioned observations of Chung et al. that increasing the Fe concentration of the electrolyte beyond a certain value had no additional benefit (they did not report Ni concentrations).[26] With increasing Ni/Fe ratio, the performance gradually becomes worse until there is a large deterioration at a value of around 30. This (and the results in Figure 5) indicates that the Fe dissolution/re-deposition rate is much faster than the corresponding rate of Ni, and the enhancing effect seems to saturate when the Fe concentration reaches about half of the Ni concentration. Conversely, the effect of Fe species can also be suppressed by Ni species, but only when the Ni concentration is much higher (over ~7-fold) than the Fe concentration.

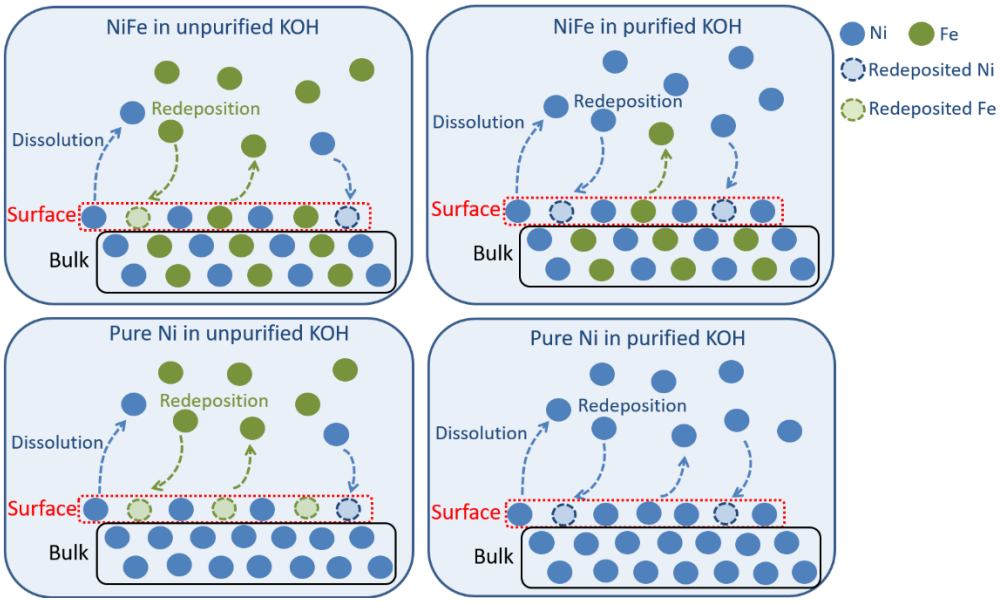

Figure 7. Schematic diagram of dissolution/re-deposition of Ni and Fe in unpurified and purified KOH electrolytes for NiFe and pure Ni films.

Based on above results and the discussions, we propose a dissolution/re-deposition mechanism for the NiFe and pure Ni films in alkaline conditions (Figure 7). First, the Raman and GIXRD results described above clearly show that only the surface of the films experiences structural transformations during the CV cycling, the bulk of the films remains unchanged. Secondly, both the soluble Fe and Ni species present in the electrolyte affect the OER activity. Specifically, the availability of Fe in electrolyte is important and necessary for both NiFe and pure Ni to

obtain (and also to maintain) enhanced OER activity, while the presence of Ni in the electrolyte is detrimental to the OER.[31] Thirdly, the impacts of soluble Fe and Ni in the KOH on the OER activity are determined by their relative concentrations (i.e. Ni/Fe, or Fe/Ni ratio). For NiFe films in unpurified KOH, both the Ni and Fe on the surface of NiFe dissolve into the electrolyte during the CV cycling or OER. However, since the unpurified KOH itself contains Fe, the surface concentration of Fe can be maintained via the Fe re-deposition process. In purified KOH, however, there are almost no Fe impurities in the electrolyte, hence the empty lattice sites from the dissolved Fe ions are occupied by the Ni ions via the Ni re-deposition. This explains the relatively poor OER activity and lower I_{557}/I_{480} ratio value of NiFe in the purified KOH electrolyte. For the pure Ni film in unpurified electrolyte, Fe from the electrolyte is deposited on the surface, which explains why the corresponding I_{557}/I_{480} ratio and OER activity of the pure Ni films after 200 CV cycles is similar to that of the NiFe films in unpurified KOH. Finally, the pure Ni films exhibit poor OER performance in purified KOH due to the very low Fe impurity concentration in the KOH.

3.4 Stability under continuous and intermittent OER operations

The stability of the electrocatalysts is one of the most important practical concerns for water splitting. The stability measurement was first conducted on the NiFe and pure Ni films under continuous OER operation. The previous results indicate that the CV activation could improve the OER activity due to the incorporation of Fe from the KOH. Therefore, in order to eliminate uncertainties, all the stability measurements were performed after 200 CV cycles.

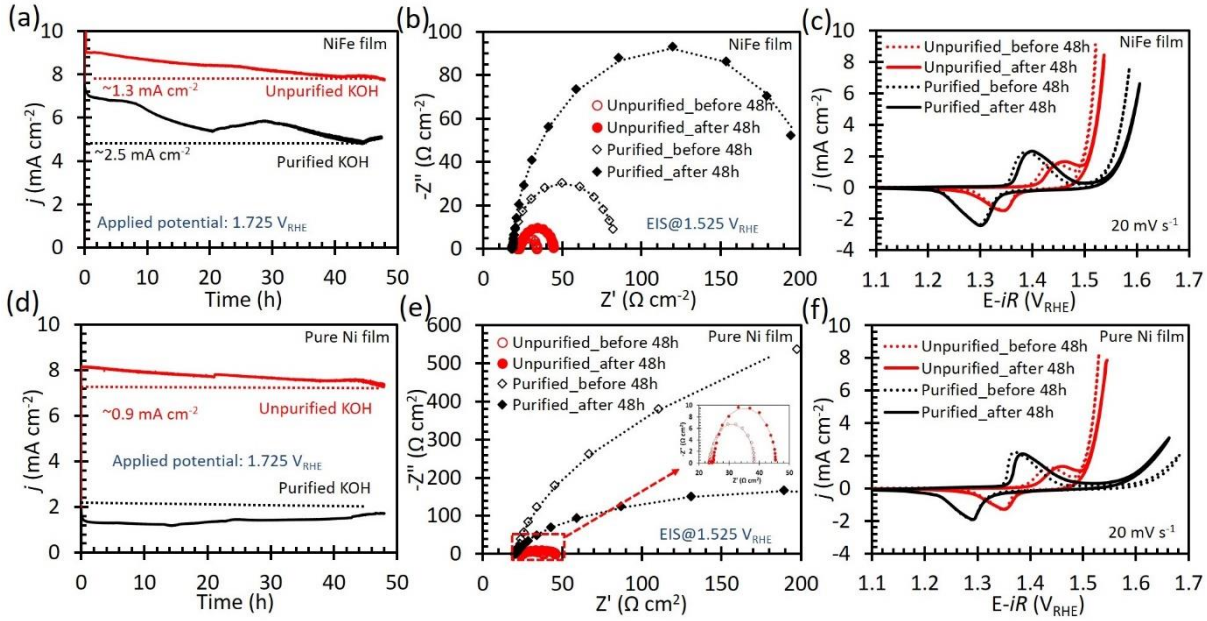

Figure 8. Stability results of NiFe film (a–c) and pure Ni film (e–f) in unpurified and purified KOH under continuous OER operation (1.725 V_{RHE}).

Figures 8a–c show the stability results of the NiFe film collected under continuous OER operation at an applied potential of 1.725 V_{RHE} for 48 h. We selected this bias potential because it generates around 10 mA cm^{-2} current density with the NiFe film. The figure shows that the NiFe film in unpurified KOH is not stable under these conditions and the obtained current density decays by 1.3 mA cm^{-2} during the 48 h, i.e., from 9.1 mA cm^{-2} to 7.8 mA cm^{-2}. This observation is consistent with the literature that NiFe-based electrocatalysts are not stable under prolonged continuous OER operating conditions.[20,22,43] Compared to unpurified KOH, NiFe films in purified KOH degraded more severely, from 7.4 mA cm^{-2} to 5.2 mA cm^{-2} (black curve in Figure 8a). Based on the dissolution/re-deposition mechanism described above, we propose that during the OER operation the surface Fe sites of the NiFe film are gradually replaced by Ni species in the purified KOH (due to relatively low Fe concentration and relatively high Ni concentration). The electrochemical impedance spectra (EIS) and CV results in Figure 8b–c as well as Table S2 further confirm the catalyst deactivation (details about the EIS fitting can be found in Supporting Information). The fitted charge transfer resistance (R_{ct}, Ω cm^2) and time constant (τ, s**)** values for both conditions significantly increased, indicating that the barrier for the electron transfer increased greatly.[63] The derived double-layer capacitance (C_{dl}) values reduced almost by half, suggesting a decrease in the number of active surface sites. However, the change in the surface Fe content in the NiFe film is unlikely to be the reason for the OER deactivation. The XPS results show that after 48 h continuous OER operation in unpurified KOH, the Fe composition (Fe/(Fe+Ni)) increases from 18.7 at.% to 26.5 at.% (Figure S8). It is noticeable that the size of the redox feature for both cases (unpurified and purified KOH) before and after 48 h OER operation remains almost unchanged, indicating that the total $Ni(OH)_2$/NiOOH content did not change during this period. These results imply that the increase in Fe content during the continuous OER operation does not improve the OER activity. In addition, the GIXRD data (Figure S6) collected after 48 h continuous OER for NiFe in unpurified KOH show that the bulk of the film still remains present as a metallic phase.

As a comparison, the stability of the pure Ni film in unpurified KOH and purified KOH electrolytes was also measured by the same protocol as NiFe film (Figures 8e–f). Similarly to NiFe film in unpurified KOH, the current density of the pure Ni film decayed over time. The corresponding EIS and CV exhibit the same trend as observed for NiFe film in unpurified KOH. The similarity between the NiFe and Ni films is not unexpected, since the surface of the pure

Ni film is also expected to contain Fe after prolonged cycling in the unpurified electrolyte. In contrast, the behavior in purified KOH is very different, with no degradation occurring for the pure Ni films. Note that the OER activity of these films is poor due to the absence of Fe in both the film and the electrolyte.[64] Surprisingly, the OER activity slightly increases after the 48 h stability measurement. Table S2 demonstrates that in purified KOH the C_{dl} decreases from 2.4 to 1.7 mF cm^{-2}, with the R_{ct} value simultaneously decreasing from 2339 Ω cm^2 to 377 Ω cm^2. These results imply that the slight OER improvement for the pure Ni film in purified KOH after 48 h was not due to an increase in the active surface area (it actually decreases). Figure 8f shows that the Ni^{2+}/Ni^{3+} redox peak shifts to slightly more anodic potentials after cycling. All these observations are consistent with the presence of trace Fe impurities in the purified KOH, which can enhance the OER activity but also block part of the Ni surface sites.[65]

The Raman spectra for NiFe and pure Ni films before and after the 48 h continuous operation in unpurified and purified KOH were also measured and compared (Figure S7). The I_{557}/I_{480} ratio increases slightly after the stability tests in unpurified KOH (Figures S7a and S7c), from 0.92 to 0.99 for NiFe and 0.96 to 0.99 for pure Ni. This small increase hints at increased structural disorder, likely caused by an increased surface Fe content (see the XPS results in Figure S8). In purified KOH electrolyte, however, the I_{557}/I_{480} ratio of NiFe remained almost unchanged after 48 h continuous OER operation (Figure S7b). This is because the Fe has already leached out before the start of the 48h measurement, and is not re-deposited in the purified KOH electrolyte. The slight decrease of the I_{557}/I_{480} ratio from 0.71 to 0.65 can be ascribed to the increased NiOOH content. The difference between the NiFe and pure Ni in purified KOH is that the pure Ni film does not contain any Fe originally; therefore, the NiOOH content increases with the continuous OER operation.

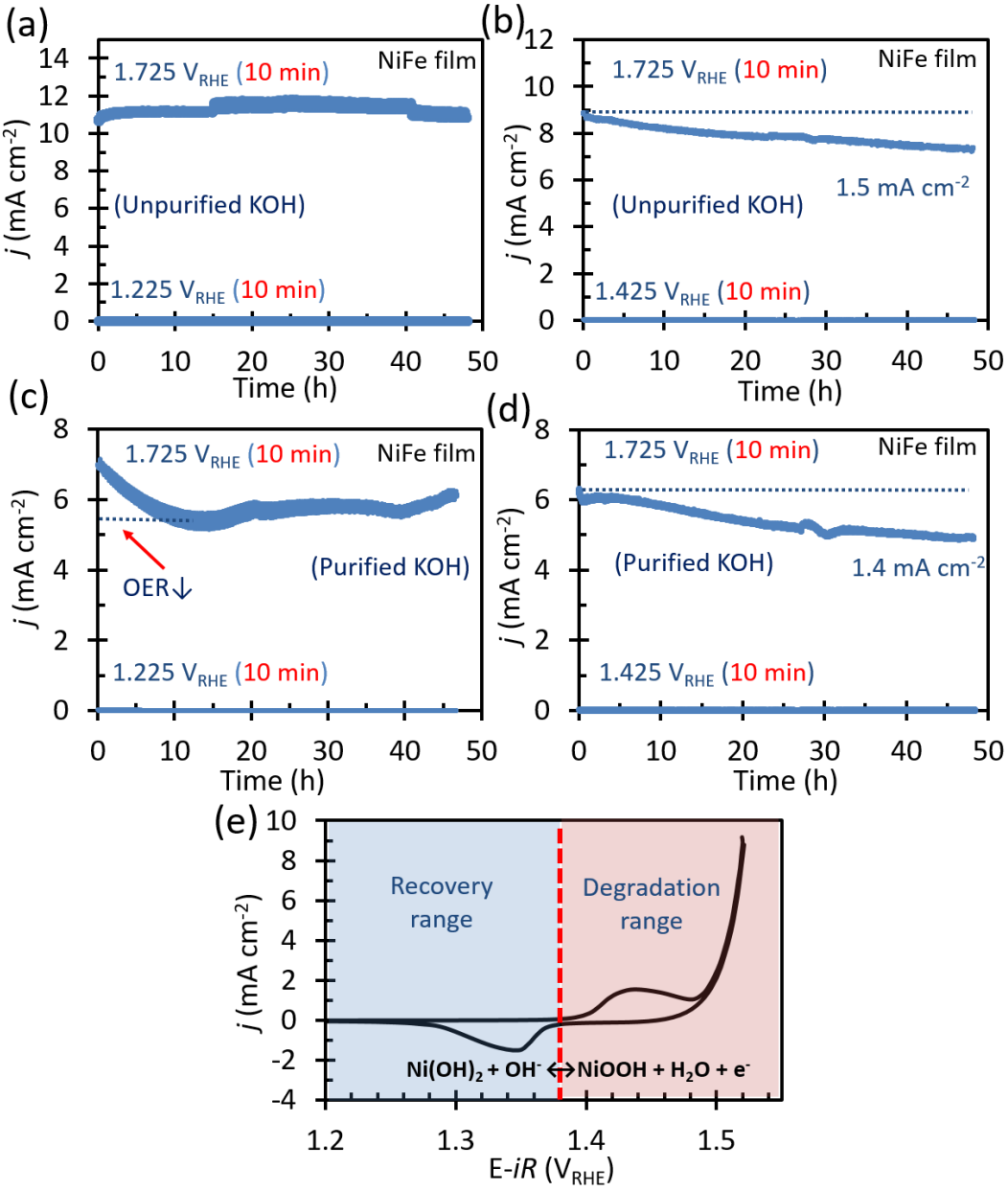

Figure 9. Stability results of a NiFe film in unpurified 1.0 M KOH (a) and purified 1.0 M KOH (c) under intermittent operating conditions (cycling between 1.725 V_{RHE} (10 min) and 1.225 V_{RHE} (10 min)) for 48 h; stability results of NiFe film in unpurified 1.0 M KOH (b) and purified 1.0 M KOH (d) under intermittent operating conditions (cycling between 1.725 V_{RHE} (10 min) and 1.425 V_{RHE} (10 min)) for 48 h; (e) Proposed explanation to the OER degradation.

The above results indicate that the NiFe films are not stable under prolonged continuous OER conditions. We were curious about their stability under fluctuating OER operations, since photoelectrochemical (PEC) devices and PV-driven electrolysers (PV-EC) would inevitably operate under intermittent conditions.[54,66] Figure 9a illustrates the results of a further stability test in an unpurified electrolyte using a slightly different testing protocol to imitate intermittent

operating conditions. First, the potential was fixed at 1.725 V_{RHE} for 10 min and 1.225 V_{RHE} for another 10 min, and then repeating this process for 48 h. Interestingly, no obvious OER degradation is observed. The corresponding CVs (see Figure 11) show that the OER activity after the 48 h has improved. However, if the potential is cycled to 1.425 V_{RHE} instead of 1.225 V_{RHE} (Figure 8b), the OER degradation occurred again (1.5 mA cm^{-2} decrease in 48 h). Notably, both 1.225 and 1.425 V_{RHE} are negative of the OER on-set potential (~1.50 V_{RHE}), but 1.225 V_{RHE} is less anodic while 1.425 V_{RHE} is more anodic than the reduction potential of NiOOH→$Ni(OH)_2$ (~1.35 V_{RHE}). These results suggest that the conversion of NiOOH to $Ni(OH)_2$ is conducive to maintaining the OER activity. We also conducted a stability measurement on the NiFe film in purified KOH under intermittent OER operating conditions (Figure 8c). During the first 15 h, the NiFe film suffers from deactivation, which could be due to the Fe sites on the film surface being replaced by the Ni ions during the dissolution/re-deposition process, as discussed related to Figure 7. However, after 15 h the OER performance of NiFe film does not decrease further, similar to the observation in Figure 8d. Figure 9d shows the stability results of NiFe film by using the same test protocol as Figure 9b, but performed in purified KOH. Unlike the results in Figure 9c, NiFe film undergoes a continuous OER decay over time, which is similar to the results in Figure 8a and further demonstrates the importance of converting NiOOH to $Ni(OH)_2$ for maintaining OER stability.

Based on the stability results above, it seems that there are two important potential ranges which determine the OER stability of the NiFe, i.e. the ranges cathodic and anodic of the Ni reduction potential (called here “recovery range” and “degradation range”, respectively, as shown in Figure 9e). When the NiFe-based electrocatalysts are exposed to OER conditions for a period of time, it is important to periodically change the applied potential to the recovery range, where the catalyst can recover its lost OER activity. The border between these two ranges is determined by the Ni redox profile of the electrocatalysts, i.e. the applied potential should be low enough to reduce the NiOOH to $Ni(OH)_2$.

To verify the mechanism proposed above, the NiFe film was measured under accelerated stress test (AST) conditions, i.e., 10 min at the potential of 1.725 V_{RHE}, then 10 min at the potential of 1.575 V_{RHE}, and then the OCP for another 10 min. The total duration time for the measurement was 96 h. This AST protocol has been employed to evaluate the stability of electrocatalysts in proton exchange membrane (PEM) water electrolyzers.[67,68] It is useful also for testing NiFe-based electrocatalysts, because its operating conditions are closer to real-life operation in PEC and PV-EC devices than simple chronopotentiometry or chronoamperometry.

As shown in Figure S10a and Table S3, the NiFe film does not show any OER performance deactivation during the 96 h measurement period. Actually, its OER activity improves a little after the stability tests, which is further confirmed by EIS and CV results in Figure S10b and S10c. We notice that during the stability measurements the OCP value was located within the range 1.125–1.325 V_{RHE}, which corresponds to the recovery range. Thus, the key for maintaining the OER performance seems to be intermittent OCP operation. This explains the long-term stability of the film and further supports the proposed mechanism.

3.5 Explanations to the OER degradation and preservation

To understand the surface change of the NiFe film, we also collected and compared the XPS spectra after the 48 h continuous and intermittent OER operations (Figure 10). The XPS spectra of Ni $2p_{3/2}$ for both cases can be fitted with two characteristic peaks at 855.1 and 856.2 eV, which are associated with the formation of $Ni(OH)_2$ and NiOOH, respectively.[69] Such results are consistent with the Raman spectra in Figure S6 in which the NiOOH phase is present. It is noticeable that the surface NiOOH content (25.1%) after the continuous operation is much higher than that after intermittent operation (7.7%). These results confirm the hypothesis that a high content of NiOOH is unfavorable to maintaining the OER activity. However, it must be pointed out that the high content of NiOOH is unlikely to be the direct cause for the OER degradation because the pure Ni film did not show any OER deactivation in purified KOH after 48 h continuous OER operation (Figure 8d).

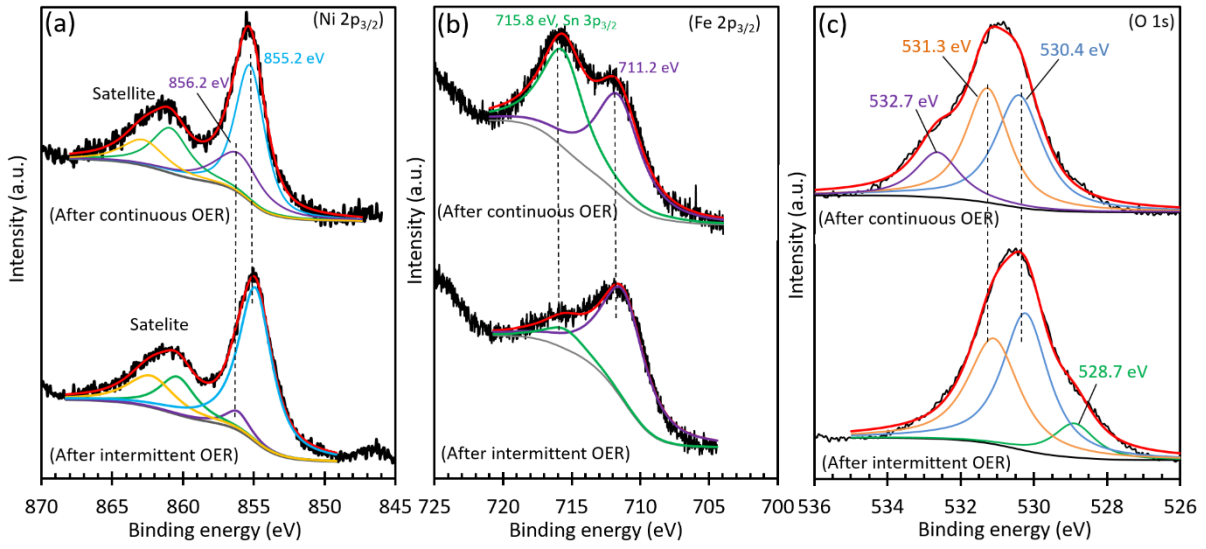

Figure 10. XPS spectra of Ni $2p_{3/2}$ (a), Fe $2p_{3/2}$ (b) and O 1s (c) of NiFe films in unpurified KOH after 48h under continuous OER operating conditions and after 48h under intermittent OER operating conditions.

The characteristic Fe $2p_{3/2}$ peak located at 711.2 eV indicates the generation of iron oxides and/or (oxy)hydroxides.[70] Due to the partial overlap with Sn $3p_{3/2}$ (715.8 eV) and the complexity of iron phases, it is difficult to assign the signal at 711.2 eV to any single phase of iron.[71] Still, the surface Fe content after the prolonged OER operations can be calculated. As shown in Figure S8, the relative Fe content (i.e., Fe/(Fe+Ni)) after 48 h continuous and intermittent OER operations increases from 18.7 at.% to 26.5 at.% and 22.5%, respectively. These results indicate that the NiFe film continuously incorporates Fe species from the unpurified KOH during the OER catalysis, which increases the Fe/Ni ratio on the film surface. However, several articles report that Fe leaches from the parent NiFe-based electrocatalysts into the alkaline electrolyte during the OER catalysis.[21,22,26] For example, Görlin *et al.* observed, via reflection X-ray fluorescence spectroscopy, a great loss of Fe from a Ni-Fe oxy-hydroxide film after 2 h OER operation in purified KOH.[72] We note that the OER measurements on the NiFe-based electrocatalysts in these references (i.e.[21,22,26,72]) were conducted in purified KOH. Therefore, the loss of Fe is likely due to the Fe dissolution and the high content of Ni species in purified KOH, which occupy the Fe sites, as explained by the proposed mechanism in Figure 7. This eventually results in the deactivation of the OER activity. In contrast, we observe an increase in Fe because the Fe content exceeds the Ni content in our unpurified electrolyte (Table S1). Figure 10c compares the XPS spectra of O 1s of NiFe film collected after the 48 h continuous and 48 h intermittent operations in unpurified KOH. The peaks at 530.4 eV and 531.3 eV can be ascribed to the oxide and hydroxyl groups of the NiFe alloy, respectively.[62] Additionally, the appearance of the bond at 532.7 eV after continuous OER operation can be attributed to chemically adsorbed water molecules,[10] which could originate from the intercalation of H_2O molecules into the layers of γ-NiOOH.[44] The peak at 528.7 eV for the intermittent conditions is ascribed to the lattice oxygen (O^{2-}) in the layered structure.[60] These results further indicate that continuous operation enhances the formation of NiOOH.

The CV curves of the NiFe film recorded for both continuous and intermittent operation are also compared. As shown in Figure 11, the area of the Ni^{2+}/Ni^{3+} redox peaks for continuous OER operation did not change significantly after operation, but the anodic peak slightly shifted towards more positive potentials. For intermittent operation the area of the redox peak increased greatly and both the cathodic and anodic peaks shifted to more anodic potential, implying that more $Ni(OH)_2$/NiOOH was generated and that the NiFe film was further activated under the intermittent OER operation. Therefore, the potential shifts between the "degradation" and "recovery" ranges during the 48 h intermittent operation are similar to the CV cycling, which further improves the OER activity. Since we previously showed that the increase in

$Ni(OH)_2$/NiOOH content alone does not have a direct relationship with the OER activity, the improvement after intermittent operation is caused by the increased Fe content. However, it is noticeable from XPS that the surface Fe content after the continuous OER operation also increased but its OER performance degraded. This result contradicts several previous observations that the Fe content in the NiFe-based electrocatalysts decreases.[20–22] Therefore, we propose that during OER operation Fe is converted likely to FeOOH, and its accumulation in continuous operation reduces the OER activity, while under intermittent operation the FeOOH is removed periodically, so the catalyst activity remains more stable.[29] In addition, the SEM images (Figure S9) collected before and after the 48 h continuous OER operation (applied potential 1.725 V_{RHE}) show that the morphology of the NiFe film remained almost intact, indicating the good stability of the film.

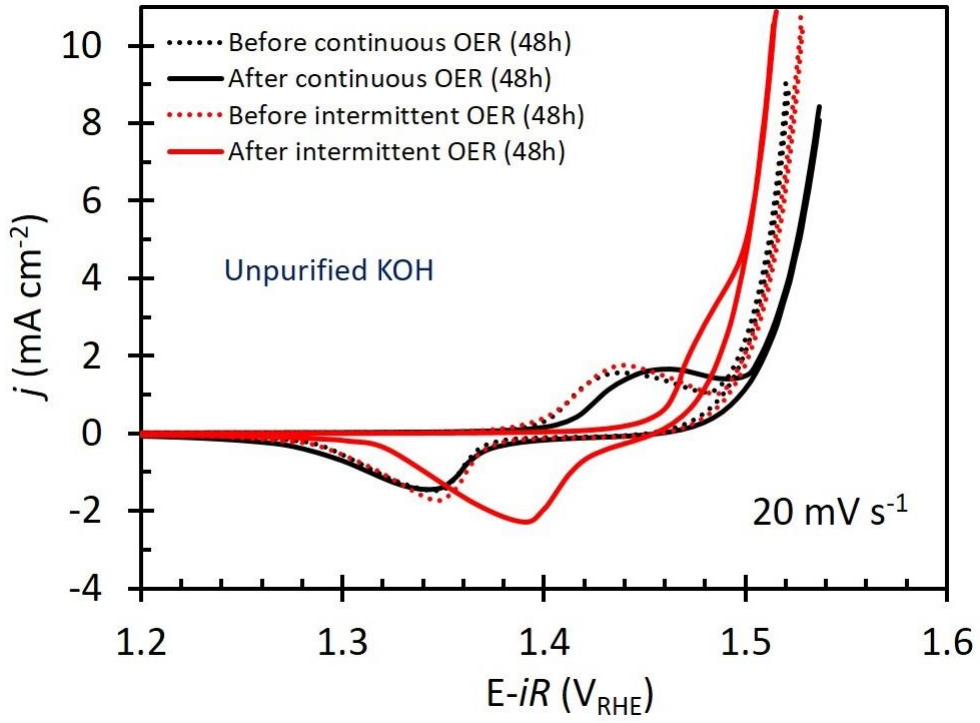

Figure 11. CV curves of a NiFe film recorded before and after the 48 h continuous (black curves) and intermittent (red curves) OER operations in unpurified KOH.

Previously Mellsop *et al.* studied the OER stability of Ni oxy-hydroxide in 30 wt.% KOH.[73] They attributed the OER degradation under prolonged continuous OER operation to the increasing ratio of Ni(IV) to Ni(III). To prevent the formation of Ni(IV), they proposed a rejuvenation operation by holding the electrode at a lower potential range of 0.5–0.36 V vs Hg/HgO (~1.4–1.5 V_{RHE}) and argued that it is key to avoid the reduction of Ni(III) to Ni(II). However, these conclusions conflict with our results which indicate that, in fact, the reduction

of Ni(III) to Ni(II) is the key to maintaining the OER activity. Furthermore, they did not mention the KOH purity, which is important to the stability, as illustrated by pure Ni film in purified KOH not showing activity degradation after prolonged OER operation, while in unpurified KOH its activity was degraded (Figure 8d). Kaui *et al.* recently found that the formation of FeOOH caused by the Fe segregation is responsible for the OER degradation of the mixed Ni-Fe hydroxide under prolonged continuous OER operation.[29] They proposed that the phase segregation can be alleviated by holding the electrode at a reduction state intermittently. Although we were not able to identify the FeOOH phase in our current study, our results suggest that the increase in NiOOH content under prolonged continuous OER is likely related to the formation of FeOOH. Obviously, the reduction of the NiOOH to $Ni(OH)_2$ by CV cycling or intermittent operations are conducive to maintaining (and even improving) the OER activity.

4. Conclusions

In summary, we have reported the effects of Fe on the surface structure evolution and the OER activity of metallic NiFe (and pure Ni) films in alkaline electrolyte. The film surface evolves from metallic Ni^0/NiO/$Ni(OH)_2$ to $Ni(OH)_2$/NiOOH during electrochemical activation and the presence of Fe in KOH alters the film surface by increasing the structural disorder. Although the generation of $Ni(OH)_2$/NiOOH does not directly contribute to the OER activity of NiFe and pure Ni films, its presence enhances the Fe incorporation from the Fe-containing KOH electrolyte. In addition, the co-electrodeposited Fe in the film is not necessary because it is the surface Fe rather than the bulk Fe that is responsible for the enhanced OER activity. The analysis of the Fe and Ni species present in the KOH shows that the availability of Fe in KOH is necessary for both pure Ni and NiFe films to obtain enhanced OER activity, while the presence of Ni in the electrolyte is detrimental to the OER. The specific impacts of soluble Fe and Ni species in the electrolyte on the OER activity depend on their relative concentrations. Since the Fe dissolution/re-deposition rate is much faster than that of Ni, the effect of Ni in the KOH electrolyte on NiFe or pure Ni electrocatalysts is quite easy to eliminate by increasing the Fe concentration in the KOH. The enhancing effect of Fe saturates when its concentration reaches about half of the Ni concentration. The investigation of the OER stability shows that the OER degradation occurs as a common feature for NiFe-based materials under prolonged continuous OER operation. Surprisingly, the OER activity can be maintained for at least 48 h under intermittent OER operation. The comparison of the stability results of 48 h continuous and intermittent OER operation indicates that the increase in surface Fe content does not necessarily improve the OER activity. Two potential ranges, apparently divided by the

$Ni(OH)_2$/NiOOH redox potential, that we call OER degradation range and recovery range, are proposed to explain the OER degradation and recovery. Compared to the prolonged intermittent OER operation, the prolonged continuous OER operation generates more NiOOH that likely enhances the formation of FeOOH, eventually leading to the OER deactivation. Importantly for the application in solar driven devices, the electrode works in the recovery range for a period of the daily cycle, i.e., at night the electrode operates at a sufficiently low reduction potential to reduce Ni^{3+} to Ni^{2+}, the OER activity can be maintained (and even improved).

Conflict of Interest

The authors declare no conflict of interest.

Acknowledgements

This research was done under the PECSYS project. The project has received funding from the FUEL CELLS AND HYDROGEN 2 JOINT UNDERTAKING under grant agreement No. 735218. This Joint Undertaking receives support from the EUROPEAN UNION'S HORIZON 2020 RESEARCH AND INNOVATION programme and Hydrogen Europe and N.ERGHY. The project started on the 1st of January 2017 with a duration of 48 months. The authors acknowledge support from the Federal Ministry of Education and Research in the framework of the project Catlab (03EW0015A). R.W. and N. M. acknowledge financial support by the German Federal Ministry for Economic Affairs and Energy in the frame of the speedCIGS project (contract number 0334095E). The analysis of the electrolyte was carried out at the Solar Fuels Testing Facility which was supported by the Helmholtz Energy Materials Foundry (HEMF) funded by the Helmholtz Association.

References:

(1) Faber, M. S.; Jin, S. Earth-Abundant Inorganic Electrocatalysts and Their Nanostructures for Energy Conversion Applications. *Energy Environ. Sci.* **2014**, *7*, 3519–3542.

(2) Callejas, J. F.; Read, C. G.; Roske, C. W.; Lewis, N. S.; Schaak, R. E. Synthesis, Characterization, and Properties of Metal Phosphide Catalysts for the Hydrogen-Evolution Reaction. *Chem. Mater.* **2016**, *28*, 6017–6044.

(3) Zhang, J.; Liu, J.; Xi, L.; Yu, Y.; Chen, N.; Sun, S.; Wang, W.; Lange, K. M.; Zhang, B. Single-Atom Au/NiFe Layered Double Hydroxide Electrocatalyst: Probing the Origin of Activity for Oxygen Evolution Reaction. *J. Am. Chem. Soc.* **2018**, *140*, 3876–3879.

(4) Zhao, S.; Yan, L.; Luo, H.; Mustain, W.; Xu, H. Recent Progress and Perspectives of Bifunctional Oxygen Reduction/Evolution Catalyst Development for Regenerative Anion Exchange Membrane Fuel Cells. *Nano Energy* **2018**, *47*, 172–198.

(5) Weng, B.; Xu, F.; Wang, C.; Meng, W.; Grice, C. R.; Yan, Y. A Layered Na 1−x Ni y Fe 1−y O 2 Double Oxide Oxygen Evolution Reaction Electrocatalyst for Highly Efficient Water-Splitting. *Energy Environ. Sci.* **2017**, *10*, 121–128.

(6) Roy, C.; Sebok, B.; Scott, S. B.; Fiordaliso, E. M.; Sørensen, J. E.; Bodin, A.; Trimarco, D. B.; Damsgaard, C. D.; Vesborg, P. C. K.; Hansen, O.; Stephens, I. E. L.; Kibsgaard, J.; Chorkendorff, I. Impact of Nanoparticle Size and Lattice Oxygen on Water Oxidation on NiFeOxHy. *Nat. Catal.* **2018**, *1*, 820–829.

(7) Görlin, M.; Ferreira de Araújo, J.; Schmies, H.; Bernsmeier, D.; Dresp, S.; Gliech, M.; Jusys, Z.; Chernev, P.; Kraehnert, R.; Dau, H.; Strasser, P. Tracking Catalyst Redox States and Reaction Dynamics in Ni–Fe Oxyhydroxide Oxygen Evolution Reaction Electrocatalysts: The Role of Catalyst Support and Electrolyte PH. *J. Am. Chem. Soc.* **2017**, *139*, 2070–2082.

(8) Xiao, H.; Shin, H.; Goddard, W. A. Synergy between Fe and Ni in the Optimal Performance of (Ni,Fe)OOH Catalysts for the Oxygen Evolution Reaction. *Proc. Natl. Acad. Sci.* **2018**, *115*, 5872–5877.

(9) Song, F.; Bai, L.; Moysiadou, A.; Lee, S.; Hu, C.; Liardet, L.; Hu, X. Transition Metal Oxides as Electrocatalysts for the Oxygen Evolution Reaction in Alkaline Solutions: An Application-Inspired Renaissance. *J. Am. Chem. Soc.* **2018**, *140*, 7748–7759.

(10) Loos, S.; Zaharieva, I.; Chernev, P.; Lißner, A.; Dau, H. Electromodified NiFe Alloys as Electrocatalysts for Water Oxidation: Mechanistic Implications of Time-Resolved UV/Vis Tracking of Oxidation State Changes. *ChemSusChem* **2019**, *12*, 1966–1976.

(11) Kim, K. H.; Zheng, J. Y.; Shin, W.; Kang, Y. S. Preparation of Dendritic NiFe Films by Electrodeposition for Oxygen Evolution. *RSC Adv.* **2012**, *2*, 4759–4767.

(12) Yu, X.; Yang, P.; Chen, S.; Zhang, M.; Shi, G. NiFe Alloy Protected Silicon Photoanode for Efficient Water Splitting. *Adv. Energy Mater.* **2017**, *7*, 1601805.

(13) Potvin, E.; Brossard, L. Electrocatalytic Activity of Ni-Fe Anodes for Alkaline Water Electrolysis. *Mater. Chem. Phys.* **1992**, *31*, 311–318.

(14) Gao, Z.; Liu, J.; Chen, X.; Zheng, X.; Mao, J.; Liu, H.; Ma, T.; Li, L.; Wang, W.; Du, X. Engineering NiO/NiFe LDH Intersection to Bypass Scaling Relationship for Oxygen Evolution Reaction via Dynamic Tridimensional Adsorption of Intermediates. *Adv. Mater.* **2019**, *31*, 1804769.

(15) Chen, J. Y. C.; Dang, L.; Liang, H.; Bi, W.; Gerken, J. B.; Jin, S.; Alp, E. E.; Stahl, S. S. Operando Analysis of NiFe and Fe Oxyhydroxide Electrocatalysts for Water Oxidation: Detection of Fe 4+ by Mössbauer Spectroscopy. *J. Am. Chem. Soc.* **2015**, *137*, 15090–15093.

(16) Gong, M.; Dai, H. A Mini Review of NiFe-Based Materials as Highly Active Oxygen Evolution Reaction Electrocatalysts. *Nano Res.* **2015**, *8*, 23–39.

(17) Im, S. W.; Ahn, H.; Park, E. S.; Nam, K. T.; Lim, S. Y. Electrochemically Activated NiFeO x H y for Enhanced Oxygen Evolution. *ACS Appl. Energy Mater.* **2021**, *4*, 595–601.

(18) Singh, R. N.; Pandey, J. P.; Anitha, K. L. Preparation of Electrodeposited Thin Films of Nickel-Iron Alloys on Mild Steel for Alkaline Water Electrolysis. Part I: Studies on Oxygen Evolution. *Int. J. Hydrogen Energy* **1993**, *18*, 467–473.

(19) Etzi Coller Pascuzzi, M.; Man, A. J. W.; Goryachev, A.; Hofmann, J. P.; Hensen, E. J. M. Investigation of the Stability of NiFe-(Oxy)Hydroxide Anodes in Alkaline Water Electrolysis under Industrially Relevant Conditions. *Catal. Sci. Technol.* **2020**, *10*, 5593–5601.

(20) Lee, S.; Cho, H.-S.; Cho, W.-C.; Kim, S.-K.; Cho, Y.; Kim, C.-H. Operational Durability of Three-Dimensional Ni-Fe Layered Double Hydroxide Electrocatalyst for Water Oxidation. *Electrochim. Acta* **2019**, *315*, 94–101.

(21) Speck, F. D.; Dettelbach, K. E.; Sherbo, R. S.; Salvatore, D. A.; Huang, A.; Berlinguette, C. P. On the Electrolytic Stability of Iron-Nickel Oxides. *Chem* **2017**, *2*, 590–597.

(22) Obata, K.; Takanabe, K. A Permselective CeOx Coating To Improve the Stability of Oxygen Evolution Electrocatalysts. *Angew. Chemie* **2018**, *130*, 1632–1636.

(23) Moysiadou, A.; Hu, X. Stability Profiles of Transition Metal Oxides in the Oxygen Evolution Reaction in Alkaline Medium. *J. Mater. Chem. A* **2019**, *7*, 25865–25877..

(24) Feng, C.; Faheem, M. B.; Fu, J.; Xiao, Y.; Li, C.; Li, Y. Fe-Based Electrocatalysts for Oxygen Evolution Reaction: Progress and Perspectives. *ACS Catal.* **2020**, *10*, 4019–4047.

(25) Le Formal, F.; Yerly, L.; Potapova Mensi, E.; Pereira Da Costa, X.; Boudoire, F.; Guijarro, N.; Spodaryk, M.; Züttel, A.; Sivula, K. Influence of Composition on Performance in Metallic Iron–Nickel–Cobalt Ternary Anodes for Alkaline Water Electrolysis. *ACS Catal.* **2020**, *10*, 12139–12147.

(26) Chung, D. Y.; Lopes, P. P.; Farinazzo Bergamo Dias Martins, P.; He, H.; Kawaguchi, T.; Zapol, P.; You, H.; Tripkovic, D.; Strmcnik, D.; Zhu, Y.; Seifert, S.; Lee, S.; Stamenkovic, V. R.; Markovic, N. M. Dynamic Stability of Active Sites in Hydr(Oxy)Oxides for the Oxygen Evolution Reaction. *Nat. Energy* **2020**, *5*, 222–230.

(27) Deng, J.; Nellist, M. R.; Stevens, M. B.; Dette, C.; Wang, Y.; Boettcher, S. W. Morphology Dynamics of Single-Layered Ni(OH)2/NiOOH Nanosheets and Subsequent Fe Incorporation Studied by in Situ Electrochemical Atomic Force Microscopy. *Nano Lett.* **2017**, *17*, 6922–6926.

(28) Farhat, R.; Dhainy, J.; Halaoui, L. I. OER Catalysis at Activated and Codeposited NiFe-Oxo/Hydroxide Thin Films Is Due to Postdeposition Surface-Fe and Is Not Sustainable without Fe in Solution. *ACS Catal.* **2020**, *10*, 20–35.

(29) Kuai, C.; Xu, Z.; Xi, C.; Hu, A.; Yang, Z.; Zhang, Y.; Sun, C.; Li, L.; Sokaras, D.; Dong, C.; Qiao, S.; Du, X.; Lin, F. Phase Segregation Reversibility in Mixed-Metal Hydroxide Water Oxidation Catalysts. *Nat. Catal.* **2020**, *3*, 743–753.

(30) Anantharaj, S.; Karthik, P. E.; Kundu, S. Petal-like Hierarchical Array of Ultrathin Ni(OH)2nanosheets Decorated with $Ni(OH)_2$ nanoburls: A Highly Efficient OER Electrocatalyst. *Catal. Sci. Technol.* **2017**, *7*, 882–893.

(31) Ye, J.-M.; He, D.-H.; Li, F.; Li, Y.-L.; He, J.-B. Roles of Soluble Species in the Alkaline Oxygen Evolution Reaction on a Nickel Anode. *Chem. Commun.* **2018**, *54*, 10116–10119.

(32) Trotochaud, L.; Young, S. L.; Ranney, J. K.; Boettcher, S. W. Nickel-Iron Oxyhydroxide Oxygen-Evolution Electrocatalysts: The Role of Intentional and Incidental Iron Incorporation. *J. Am. Chem. Soc.* **2014**, *136*, 6744–6753.

(33) Lauermann, I.; Steigert, A. CISSY: A Station for Preparation and Surface/Interface Analysis of Thin Film Materials and Devices. *J. large-scale Res. Facil. JLSRF* **2016**, *2*, A67.

(34) Fu, S.; Song, J.; Zhu, C.; Xu, G.-L.; Amine, K.; Sun, C.; Li, X.; Engelhard, M. H.; Du, D.; Lin, Y. Ultrafine and Highly Disordered Ni2Fe1 Nanofoams Enabled Highly Efficient Oxygen Evolution Reaction in Alkaline Electrolyte. *Nano Energy* **2018**, *44*, 319–326.

(35) Su, C.-W.; Wang, E.-L.; Zhang, Y.-B.; He, F.-J. Ni1−xFex (0.1<x<0.75) Alloy Foils Prepared

from a Fluorborate Bath Using Electrochemical Deposition. *J. Alloys Compd.* **2009**, *474*, 190–194.

(36) Yan, W.; Li, H.; Liu, J.; Guo, J. EPMA and XRD Study on Nickel Metal Thin Film for Temperature Sensor. *Sensors Actuators A Phys.* **2007**, *136*, 212–215.

(37) Neale, A. R.; Jin, Y.; Ouyang, J.; Hughes, S.; Hesp, D.; Dhanak, V.; Dearden, G.; Edwardson, S.; Hardwick, L. J. Electrochemical Performance of Laser Micro-Structured Nickel Oxyhydroxide Cathodes. *J. Power Sources* **2014**, *271*, 42–47.

(38) Lu, Z.; Xu, W.; Zhu, W.; Yang, Q.; Lei, X.; Liu, J.; Li, Y.; Sun, X.; Duan, X. Three-Dimensional NiFe Layered Double Hydroxide Film for High-Efficiency Oxygen Evolution Reaction. *Chem. Commun.* **2014**, *50*, 6479–6482.

(39) Louie, M. W.; Bell, A. T. An Investigation of Thin-Film Ni–Fe Oxide Catalysts for the Electrochemical Evolution of Oxygen. *J. Am. Chem. Soc.* **2013**, *135*, 12329–12337.

(40) Yeo, B. S.; Bell, A. T. In Situ Raman Study of Nickel Oxide and Gold-Supported Nickel Oxide Catalysts for the Electrochemical Evolution of Oxygen. *J. Phys. Chem. C* **2012**, *116*, 8394–8400.

(41) Trześniewski, B. J.; Diaz-Morales, O.; Vermaas, D. A.; Longo, A.; Bras, W.; Koper, M. T. M.; Smith, W. A. In Situ Observation of Active Oxygen Species in Fe-Containing Ni-Based Oxygen Evolution Catalysts: The Effect of PH on Electrochemical Activity. *J. Am. Chem. Soc.* **2015**, *137*, 15112–15121.

(42) Stevens, M. B.; Enman, L. J.; Batchellor, A. S.; Cosby, M. R.; Vise, A. E.; Trang, C. D. M.; Boettcher, S. W. Measurement Techniques for the Study of Thin Film Heterogeneous Water Oxidation Electrocatalysts. *Chem. Mater.* **2017**, *29*, 120–140.

(43) Nardi, K. L.; Yang, N.; Dickens, C. F.; Strickler, A. L.; Bent, S. F. Creating Highly Active Atomic Layer Deposited NiO Electrocatalysts for the Oxygen Evolution Reaction. *Adv. Energy Mater.* **2015**, *5*, 1500412.

(44) Dionigi, F.; Strasser, P. NiFe-Based (Oxy)Hydroxide Catalysts for Oxygen Evolution Reaction in Non-Acidic Electrolytes. *Adv. Energy Mater.* **2016**, *6*, 1600621.

(45) Wu, Y.; Zhao, M.-J.; Li, F.; Xie, J.; Li, Y.; He, J.-B. Trace Fe Incorporation into Ni-(Oxy)Hydroxide Stabilizes Ni^{3+} Sites for Anodic Oxygen Evolution: A Double Thin-Layer Study. *Langmuir* **2020**, *36*, 5126–5133.

(46) Stevens, M. B.; Trang, C. D. M.; Enman, L. J.; Deng, J.; Boettcher, S. W. Reactive Fe-Sites in Ni/Fe (Oxy)Hydroxide Are Responsible for Exceptional Oxygen Electrocatalysis Activity. *J. Am. Chem. Soc.* **2017**, *139*, 11361–11364.

(47) Corrigan, D. A. The Catalysis of the Oxygen Evolution Reaction by Iron Impurities in Thin Film Nickel Oxide Electrodes. *J. Electrochem. Soc.* **1987**, *134*, 377–384.

(48) Lee, S.; Bai, L.; Hu, X. Deciphering Iron-Dependent Activity in Oxygen Evolution Catalyzed by Nickel–Iron Layered Double Hydroxide. *Angew. Chemie Int. Ed.* **2020**, *59*, 8072–8077.

(49) Burke, M. S.; Kast, M. G.; Trotochaud, L.; Smith, A. M.; Boettcher, S. W. Cobalt–Iron (Oxy)Hydroxide Oxygen Evolution Electrocatalysts: The Role of Structure and Composition on Activity, Stability, and Mechanism. *J. Am. Chem. Soc.* **2015**, *137*, 3638–3648.

(50) Song, F.; Busch, M. M.; Lassalle-Kaiser, B.; Hsu, C.; Petkucheva, E.; Bensimon, M.; Chen, H. M.; Corminboeuf, C.; Hu, X. An Unconventional Iron Nickel Catalyst for the Oxygen Evolution Reaction. *ACS Cent. Sci.* **2019**, *5*, 558–568.

(51) Chen, D.; Xiong, X.; Zhao, B.; Mahmoud, M. A.; El-Sayed, M. A.; Liu, M. Probing Structural Evolution and Charge Storage Mechanism of NiO_2H_x Electrode Materials Using In Operando Resonance Raman Spectroscopy. *Adv. Sci.* **2016**, *3*, 1500433.

(52) Klaus, S.; Cai, Y.; Louie, M. W.; Trotochaud, L.; Bell, A. T. Effects of Fe Electrolyte Impurities on Ni(OH)2/NiOOH Structure and Oxygen Evolution Activity. *J. Phys. Chem. C* **2015**, *119*, 7243–7254.

(53) Steimecke, M.; Seiffarth, G.; Bron, M. In Situ Characterization of Ni and Ni/Fe Thin Film Electrodes for Oxygen Evolution in Alkaline Media by a Raman-Coupled Scanning Electrochemical Microscope Setup. *Anal. Chem.* **2017**, *89*, 10679–10686.

(54) Kenney, M. J.; Gong, M.; Li, Y.; Wu, J. Z.; Feng, J.; Lanza, M.; Dai, H. High-Performance Silicon Photoanodes Passivated with Ultrathin Nickel Films for Water Oxidation. *Science (80-.).* **2013**, *342*, 836–840.

(55) Morales-Guio, C. G.; Mayer, M. T.; Yella, A.; Tilley, S. D.; Grätzel, M.; Hu, X. An Optically Transparent Iron Nickel Oxide Catalyst for Solar Water Splitting. *J. Am. Chem. Soc.* **2015**, *137*, 9927–9936.

(56) Grosvenor, A. P.; Biesinger, M. C.; Smart, R. S. C.; McIntyre, N. S. New Interpretations of XPS Spectra of Nickel Metal and Oxides. *Surf. Sci.* **2006**, *600*, 1771–1779.

(57) McIntyre, N. S.; Zetaruk, D. G. X-Ray Photoelectron Spectroscopic Studies of Iron Oxides. *Anal. Chem.* **1977**, *49*, 1521–1529.

(58) Grosvenor, A. P.; Kobe, B. A.; Biesinger, M. C.; McIntyre, N. S. Investigation of Multiplet Splitting of Fe 2p XPS Spectra and Bonding in Iron Compounds. *Surf. Interface Anal.* **2004**, *36*, 1564–1574.

(59) Leostean, C.; Pana, O.; Stefan, M.; Popa, A.; Toloman, D.; Senila, M.; Gutoiu, S.; Macavei, S. New Properties of Fe_3O_4@SnO_2 Core Shell Nanoparticles Following Interface Charge/Spin Transfer. *Appl. Surf. Sci.* **2018**, *427*, 192–201.

(60) Xu, X.; Song, F.; Hu, X. A Nickel Iron Diselenide-Derived Efficient Oxygen-Evolution Catalyst. *Nat. Commun.* **2016**, *7*, 1–7.

(61) Weidler, N.; Schuch, J.; Knaus, F.; Stenner, P.; Hoch, S.; Maljusch, A.; Schäfer, R.; Kaiser, B.; Jaegermann, W. X-Ray Photoelectron Spectroscopic Investigation of Plasma-Enhanced Chemical Vapor Deposited NiO x , NiOx(OH)y , and CoNiOx(OH) Y : Influence of the Chemical Composition on the Catalytic Activity for the Oxygen Evolution Reaction. *J. Phys. Chem. C* **2017**, *121*, 6455–6463.

(62) Wu, Y.; Chen, M.; Han, Y.; Luo, H.; Su, X.; Zhang, M. T.; Lin, X.; Sun, J.; Wang, L.; Deng, L.; Zhang, W.; Cao, R. Fast and Simple Preparation of Iron-Based Thin Films as Highly Efficient Water-Oxidation Catalysts in Neutral Aqueous Solution. *Angew. Chemie - Int. Ed.* **2015**, *54*, 4870–4875.

(63) Wang, J.; Xu, F.; Jin, H.; Chen, Y.; Wang, Y. Non-Noble Metal-Based Carbon Composites in Hydrogen Evolution Reaction: Fundamentals to Applications. *Adv. Mater.* **2017**, *29*, 1605838.

(64) Friebel, D.; Louie, M. W.; Bajdich, M.; Sanwald, K. E.; Cai, Y.; Wise, A. M.; Cheng, M.-J.; Sokaras, D.; Weng, T.-C.; Alonso-Mori, R.; Davis, R. C.; Bargar, J. R.; Nørskov, J. K.; Nilsson, A.; Bell, A. T. Identification of Highly Active Fe Sites in (Ni,Fe)OOH for Electrocatalytic Water Splitting. *J. Am. Chem. Soc.* **2015**, *137*, 1305–1313.

(65) Görlin, M.; Chernev, P.; Paciok, P.; Tai, C. W.; Ferreira de Araújo, J.; Reier, T.; Heggen, M.; Dunin-Borkowski, R.; Strasser, P.; Dau, H. Formation of Unexpectedly Active Ni-Fe Oxygen Evolution Electrocatalysts by Physically Mixing Ni and Fe Oxyhydroxides. *Chem. Commun.* **2019**, *55*, 818–821.

(66) Chu, S.; Majumdar, A. Opportunities and Challenges for a Sustainable Energy Future. *Nature* **2012**, *488*, 294–303.

(67) Weiß, A.; Siebel, A.; Bernt, M.; Shen, T.-H.; Tileli, V.; Gasteiger, H. A. Impact of Intermittent Operation on Lifetime and Performance of a PEM Water Electrolyzer. *J. Electrochem. Soc.* **2019**, *166*, F487–F497.

(68) Aßmann, P.; Gago, A. S.; Gazdzicki, P.; Friedrich, K. A.; Wark, M. Toward Developing Accelerated Stress Tests for Proton Exchange Membrane Electrolyzers. *Curr. Opin. Electrochem.* **2020**, *21*, 225–233.

(69) Biesinger, M. C.; Payne, B. P.; Lau, L. W. M.; Gerson, A.; Smart, R. S. C. X-Ray Photoelectron

Spectroscopic Chemical State Quantification of Mixed Nickel Metal, Oxide and Hydroxide Systems. *Surf. Interface Anal.* **2009**, *41*, 324–332.

(70) Nurlaela, E.; Shinagawa, T.; Qureshi, M.; Dhawale, D. S.; Takanabe, K. Temperature Dependence of Electrocatalytic and Photocatalytic Oxygen Evolution Reaction Rates Using NiFe Oxide. *ACS Catal.* **2016**, *6*, 1713–1722.

(71) Biesinger, M. C.; Payne, B. P.; Grosvenor, A. P.; Lau, L. W. M.; Gerson, A. R.; Smart, R. S. C. Resolving Surface Chemical States in XPS Analysis of First Row Transition Metals, Oxides and Hydroxides: Cr, Mn, Fe, Co and Ni. *Appl. Surf. Sci.* **2011**, *257*, 2717–2730.

(72) Görlin, M.; Chernev, P.; De Araújo, J. F.; Reier, T.; Dresp, S.; Paul, B.; Krähnert, R.; Dau, H.; Strasser, P. Oxygen Evolution Reaction Dynamics, Faradaic Charge Efficiency, and the Active Metal Redox States of Ni-Fe Oxide Water Splitting Electrocatalysts. *J. Am. Chem. Soc.* **2016**, *138*, 5603–5614.

(73) Mellsop, S. R.; Gardiner, A.; Marshall, A. T. Electrocatalytic Oxygen Evolution on Nickel Oxy-Hydroxide Anodes: Improvement through Rejuvenation. *Electrochim. Acta* **2015**, *180*, 501–506.

TOC:

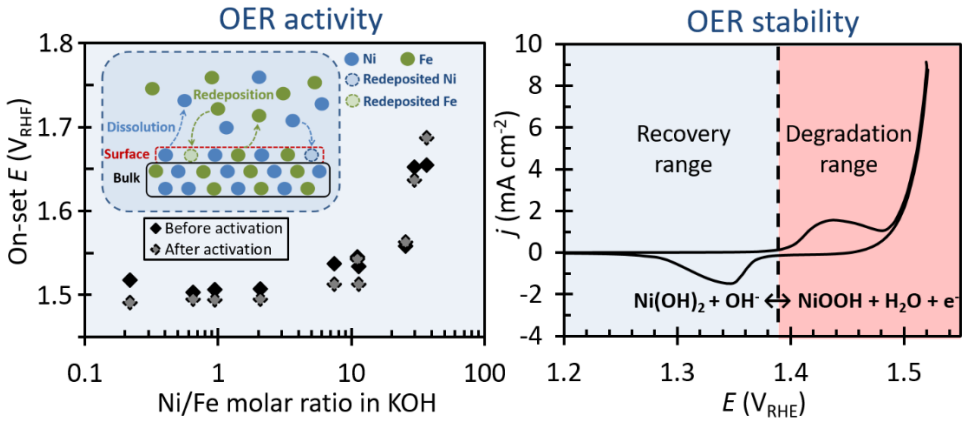
OER activity
OER stability
On-set E (V_RHF)
Ni/Fe molar ratio in KOH
Ni
Fe
Redeposited Ni
Redeposited Fe
Redeposition
Dissolution
Surface
Bulk
Before activation
After activation
j (mA cm^-2)
E (V_RHE)
Recovery range
Degradation range
Ni(OH)2 + OH- ⇔ NiOOH + H2O + e-